POLITECNICO DI TORINO

Faculty of Automotive Engineering

Masters of Automotive Engineering

Masters Thesis

Academic Year 2019-2020

GENERATION OF TOOTH PROFILE STARTING FROM CREATOR SHAPE

Supervisor:

Professor Carlo Rosso

Co-supervisors:

Mr. Fabio Bruzzone **Mr. Tomasso Maggi** **Mr. Claudio Marcellini**

Candidate:

Jean Marc Moujabber


POLITECNICO DI TORINO
1859
1906

Table of Contents

Figures Index

Tables Index

1. Introduction

Definition

Gears are machine parts used to transmit rotational motion, or torque, between two axes are known as gears. Each gear is typically circular and has teeth that operate in mesh with the teeth of a complementary gear. Teeth in mesh must have a similar shape in order to mesh properly. Gears are generally used as a simple machine to produce a change in torque, which is achieved through their gear ratio. A gear assembly with a unitary ratio can be replaced with a universal joint, or a pair of such joints if axes are to be parallel.

Two or more pairs of meshing gears are referred to as a *gear train* or *transmission*. The same meshing mechanism can combine a circular gear with a linear toothed part, a *rack*, to combine rotation with translation.

History

Gears have been in use as early as the 4th century BC in China during the late East Zhou dynasty. The oldest gears found in Europe are those of the Antikythera mechanism, designed to calculate astronomical positions, dating back to 150-100 BC. Other use of gears can be linked to Hero of Alexandria, in Roman Egypt in 50 BC, which can be traced back to the development of mechanics in the Alexandrian school in the 3rd century BC in Ptolemaic Egypt, primarily done by Archimedes (287 – 212 BC) the Greek philosopher. Examples of old gear applications include, but are not limited to:

- The Antikythera mechanism (2nd century BC)
- The South-pointing chariot of Ma Jun (200 – 265 AD)
- The mechanical clocks built in China (725 AD)
- The water-lifting device invented by Al-Jazari (1206 AD)
- The cotton gin in the Indian subcontinent (13th -14th centuries) which saw the invention of worm gears.
- The Salisbury Cathedral clock (1386 AD) rumored to have the oldest still functional geared mechanical clock.

Replacing other drive mechanisms

Gears have a similar function to *belt pulley systems*, as far as torque transmission goes. The advantages gears offer are the definite transmission ratio due to the absence of slippage and the reduced number of parts in the mechanism. The downsides are the high manufacturing cost and the lubrication requirements which result in a high operating cost per unit of time.

Material

The earliest gear material was wood, which was later replaced by nonferrous alloys, powder-metallurgy, cast irons and plastics post-industrialization. Nowadays, the most common material used is steel due to its high strength-to-weight ratio. Plastics are used in low torque applications where cost and weight can be a concern. Plastics also have the advantage of high dirt tolerance compared to steels as well as the possibility of operating without lubrication, and the reduction of repair costs. Plastic gears have been used in applications such as copy machines, printers, servo motors, and radios.

Types

A multitude of gear types exists. They can be classified according to the placement of the teeth (external – internal), the orientation of the leading edge of the teeth, or the layout of the gear axes. The following is a list of the most common gear types found in the modern industry.

- External gears: The teeth are formed on the outer surface of a cylinder or cone.
- Internal gears: The teeth are formed on the inner surface of a cylinder of cone.
- Spur gears: Straight-cut gears, which are the simplest gears of all, and commonly have an involute tooth profile.
- Helical gears: An upgrade of spur gears, with the addition of a helix angle. They allow smoother meshing and can be found in parallel or crossed orientations.
- Double helical gears: Also known as Herringbone gears. They consist of two helical gears mounted together with opposite directions to solve the axial thrust problem of helical gears.
- Bevel gears: They have a conical shape and are used to transmit rotational motion between non-parallel axes.
- Face gears: A particular type of bevel gears where the pinion is a spur gear.
- Spiral bevel gears: They have similar advantages as helical gears do to straight-cut spur gears.
- Hypoid gears: Similar to spiral bevel gears but whose axes do not intersect.
- Worm gears: They resemble screws and mesh with a worm wheel that resembles a spur gear. They typically have high gear ratios. Axes are crossed but do not intersect.
- Non-circular gears: They're characterized by a variable transmission ratio and are used for well-defined special purposes.
- Rack and pinion: It converts rotational motion to translational motion, and can be thought of a gear with infinite radius.
- Epicyclic Gears: Gear assemblies where one or more gear axes move. Examples are mechanical differentials and sun/planet gearing.

Thesis Description

In the following pages are presented the detailing of the main parameters in some of the most commonly used gears (spur, helical, face-gears), the reason involute profiles are widely standardized for gear tooth profiles, the steps of constructing the involute profile of the tooth, as well as the different gear forming techniques used in the industry. The importance of standardized tooth systems is highlighted too.

The generation by shaping of the tooth profile starting from the creator shape will then be tackled, by defining the coordinate transformation procedure coupled with an exemplary application. The types of gears that will be considered are spur gears, helical gears and face-gears.

Finally, the generation of a cloud of points representing the formed tooth profile starting from a cloud of points representing the shaper cutter is presented. The procedure exists for external spur gears, and will be modified to account for internal spur gears.

All applications in the following thesis are done on the MATLAB computer programming language, developed by MathWorks.

2. Nomenclature

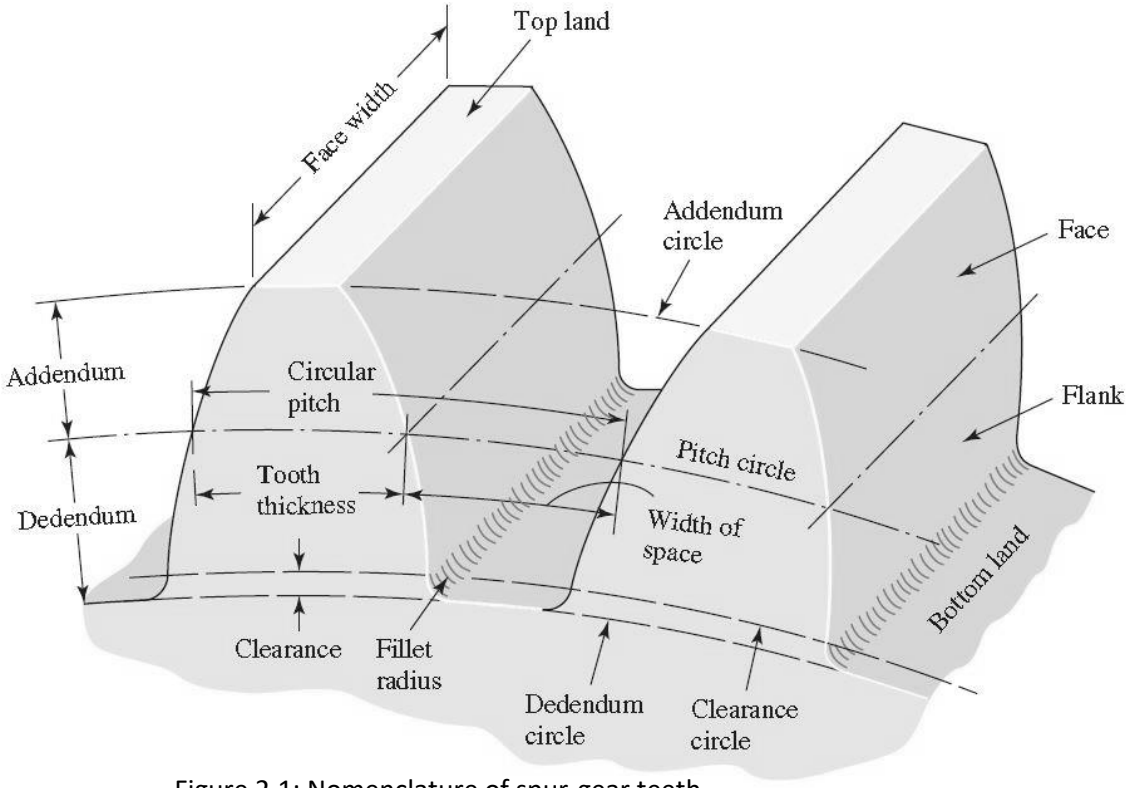

Figure 2.1: Nomenclature of spur-gear teeth

The terminology of spur gear teeth is shown in figure (2.1). The ***pitch circle*** is a theoretical circle upon which are based all calculations; its diameter is the ***pitch diameter***. The pitch circles of 2 mating gears are tangent one to the other.

The ***circular pitch p*** is the distance, from a point on one tooth to a corresponding point on an adjacent tooth. Therefore, the circular pitch is equal to the sum of the ***tooth thickness*** and the ***width of space***.

The ***module m*** is the ratio of the pitch diameter to the number of teeth. Generally, the adopted unit of length is the millimeter. The module is the index of the tooth size in SI.

The ***diametral pitch P*** is the ratio of the number of teeth on the gear to the pitch diameter. Therefore, it is the inverse of the module. It is expressed as teeth per inch.

The ***addendum a*** is the radial distance from the ***top land*** to the pitch circle. The ***dedendum b*** is the radial distance from the ***bottom land*** to the pitch circle. The whole ***depth*** h_t is the sum of the addendum and the dedendum.

The ***clearance circle*** is a circle that is tangent to the addendum circle of the mating gear. The ***clearance c*** is the amount by which the dedendum in a given gear exceeds the addendum of its mating gear. The ***backlash*** is the amount by which the *width of space* of a tooth exceeds the *tooth thickness* of the engaging tooth measured on the pitch circle.

Useful relations:

$$P = \frac{N}{d} \qquad \text{Equation 2.1}$$

$$m = \frac{d}{N} \qquad \text{Equation 2.2}$$

$$p = \frac{\pi d}{N} = \pi m \qquad \text{Equation 2.3}$$

$$pP = \pi \qquad \text{Equation 2.4}$$

Where $P =$ diametral pitch, teeth per inch.

$N =$ number of teeth.

$d =$ pitch diameter, mm or in.

$m =$ module, mm.

$p =$ circular pitch, mm or in.

3. Conjugate Action

In the following paragraphs, it is assumed that the teeth are perfectly formed, perfectly smooth and absolutely rigid. This assumption is obviously not realistic, but is adopted for the purpose of the discussion.

Mating gears teeth acting against each other to generate a rotational motion are similar to cams. When the tooth profiles, or cams, are designed to generate a constant angular velocity ratio during meshing, these are referred to as having a ***conjugate action***. In theory, at least, it is possible to draw any profile for one tooth and then to find a profile for the meshing tooth that will give a conjugate action. One of such solutions is the ***involute profile***, which, with few exceptions, is in universal use for gear teeth.

When one curved surface pushes against another (Figure 3.1), the point of contact occurs at the point of tangency (point c), and the forces at any instant are directed along the common normal ab to the two curves. The line ab, representing the direction of action of the forces, is known as the *line of action*. The line of action will intersect the line of centers *O*-*O* at some point *P*. The angular-velocity ratio between the two arms is inversely proportional to their radii to the point *P*. Circles drawn through point *P* from each center are called ***pitch circles***, and their respective radii are called the ***pitch radii***. Point *P* is the ***pitch point***.

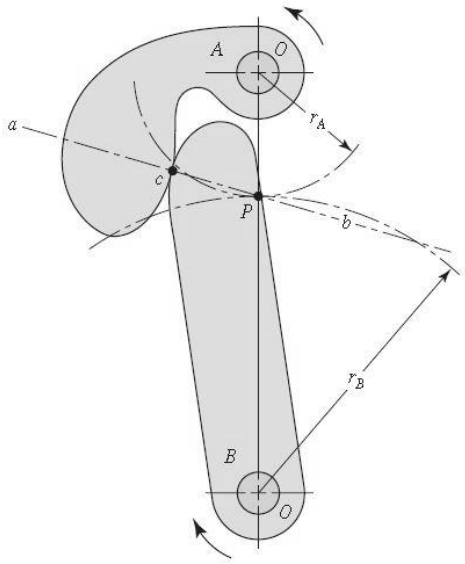

Figure 3.1: Cam A and follower B

Another observation can be made from Figure (3.1): a pair of gears is actually a set of pairs of cams that act through a small arc and, before running off the involute contour, are replaced by another identical pair of cams. The cams can run in either direction and are designed to transmit a constant angular-velocity ratio. If involute curves are used, the gears can sustain changes in center-to-center distance with *no* variation in constant angular-velocity ratio. However, the rack tooth profiles are straight-flanked, which leads to primary cutter/shaper tooling being much simpler.

To transmit motion at a constant angular-velocity ratio, the pitch point must remain fixed; that is, all the lines of action for every instantaneous point of contact must pass through the same point *P*. In the case of the involute profile, it will be shown that all points of contact occur on the same straight line *ab*, that all normals to the tooth profiles at the point of contact coincide with the line *ab*, and, thus, that these profiles transmit uniform rotary motion.

4. Involute Properties

An involute curve can be generated as evidenced in Figure (4.1). A partial flange *B* is attached to the cylinder *A*, around which is wrapped a cord *def*, which is held tight. Point *b* on the cord represents the tracing point, and as the cord is wrapped and unwrapped about the cylinder, point *b* will trace out the involute curve *ac*. The radius of the curvature of the involute varies continuously, being zero at point *a* and a maximum at point *c*. At point *b* the radius is equal to the distance *be*, since point *b* is instantaneously rotating about point *e*. Thus, the generating line *de* is normal to the involute at all points of intersection and, at the same time, is always tangent to the cylinder *A*. The circle on which the involute is generated is called ***base circle***.

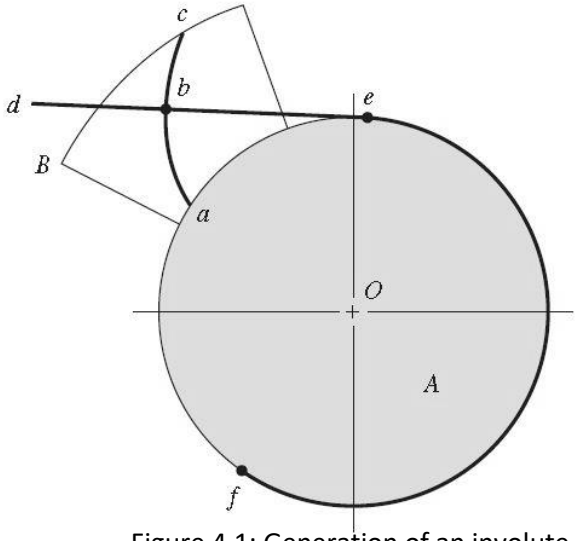

Figure 4.1: Generation of an involute

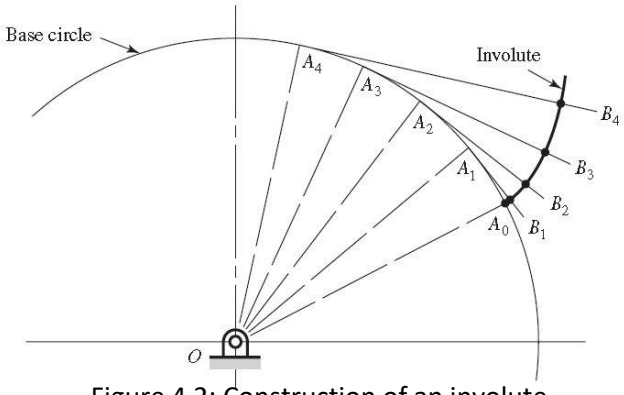

Figure 4.2: Construction of an involute

It is essential to learn how to construct an involute curve. As shown in Figure (4.2), divide the base circle into a number of equal parts, and construct radial lines OA_0 , OA_1 , OA_2 , etc. Beginning at A_1, construct perpendiculars A_1B_1, A_2B_2, A_3B_3, etc., Then along A_1B_1 lay off the distance A_1A_0, along A_2B_2 lay off twice the distance A_1A_0, etc., producing points through which the involute curve can be constructed. To investigate the fundamentals of tooth action, let us proceed step by step through the process of constructing the teeth on a pair of gears.

When two gears are in mesh, their pitch circles roll on one another without slipping. Designate the pitch radii as r_1 and r_2 and the angular velocities as ω_1 and ω_2, respectively. Then the pitch-line velocity is $V = |r_1\omega_1| = |r_2\omega_2|$.

Therefore, the relation between the radii on the angular velocities is $\left|\frac{\omega_1}{\omega_2}\right| = \left|\frac{r_2}{r_1}\right|$, and starting from this relation and the desired input and output gear velocities, a radii ratio can be found, and numbers of teeth selected accordingly.

5. Construction of a gear tooth profile

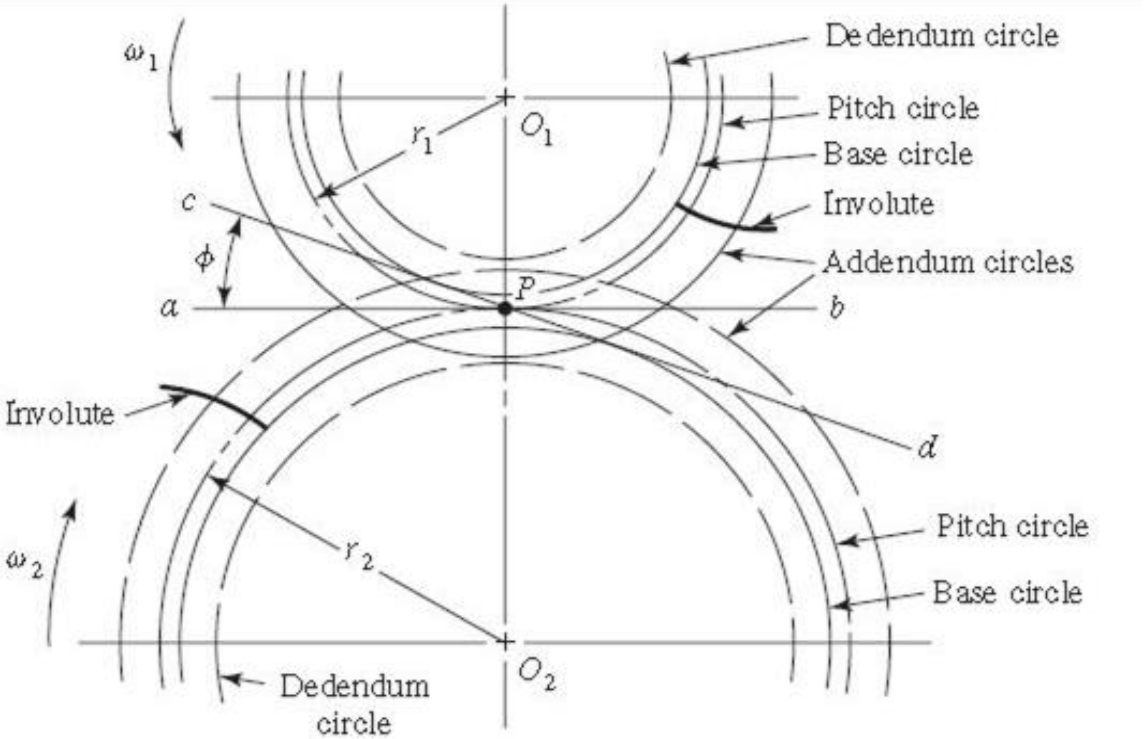

Figure 5.1: Circles of a gear layout

The primary procedure in drawing teeth on a pair of mating gears is shown in Figure (5.1). The center distance is the sum of the pitch radii, already found in previous step, and thus are located the pinion and gear centers O_1 and O_2. Then are constructed the pitch circles of radii r_1 and r_2. These are tangent at *P*, the ***pitch point***. Next is drawn the line *ab*, the common tangent, through the pitch point. Next is drawn a line *cd* through point *P* at an angle φ to the common tangent *ab*. The line *cd* has three names, all of which are in general use. It is called the ***pressure line***, the ***generating line***, and the ***line of action***. It represents the direction in which the resultant force acts between the gears. The angle φ is called ***pressure angle***, and it usually has values of 20^o or 25^o, though 14.5^o was once used. Smaller pressure angles result in lower backlash, smoother operation and less sensitivity to manufacturing errors.

Next, on each gear draw a circle tangent to the pressure line. These circles are the ***base circles***, and since they are tangent to the pressure line, the pressure angle determines their size. As shown in Figure (5.2), the radius of the base circle is $r_b = r\ cos\varphi$, where r is the pitch radius.

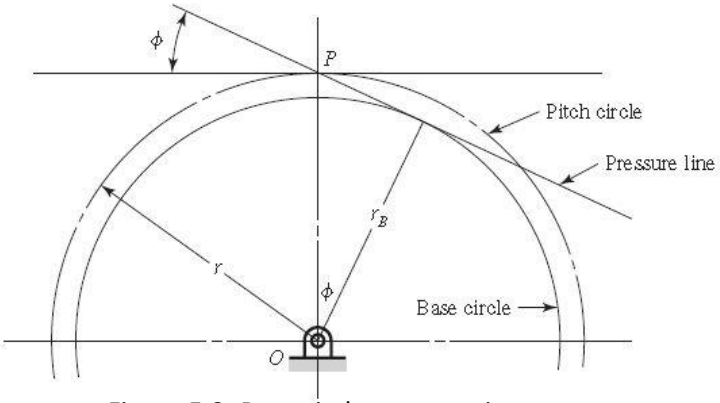

Figure 5.2: Base circle construction

Next, an involute is generated on each base circle as previously described and as shown in Figure (4.1). This involute is to be used as a template which can be turned over and replicated to obtain the other side of the tooth.

The addendum and dedendum distances for standard interchangeable teeth are, as shall be mentioned later, $1/P$ and $1.25/P$, respectively. Using these distances, the addendum and dedendum circles on the pinion and the gear can be drawn as shown in Figure (5.1).

To draw a tooth, tooth thickness must be known. From equation (2.4), the circular pitch is $p = \frac{\pi}{P}$

Therefore, the tooth thickness is $t = \frac{p}{2} = \frac{\pi}{2P}$ measured on the pitch circle.

Using this distance for the tooth thickness as well as the tooth space, it is possible to draw as many teeth as desired. Trouble could arise when drawing these teeth if one of the base circles happens to be larger than the dedendum circle. The reason for this is that the involute begins at the base circle and is undefined below this circle. So, in drawing gear teeth, a radial line is usually drawn for the profile below the base circle. The actual shape, however, will depend upon the kind of machine tool used to form the teeth in manufacture, that is, how the profile is generated.

The portion of the tooth between the clearance circle and the dedendum circle includes a fillet. Clearance corresponds to the amount by which the dedendum in a given gear exceeds the addendum of its mating gear $c = b - a$. The construction is finished when these fillets have been drawn. The results are shown in Figure (5.3).

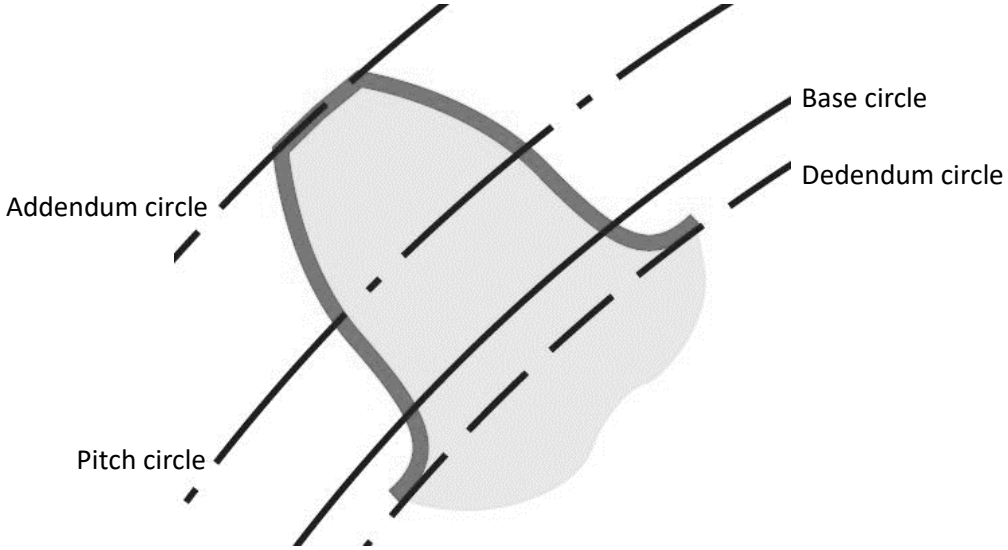

Figure 5.3: Tooth profile construction

6. Gear Forming

Numerous ways exist for forming the gear teeth, such *die casting*, *investment casting*, *sand casting*, *shell molding*, *permanent-mold casting*, and *centrifugal casting*. Teeth forming can also be done by using the *powder-metallurgy process*, or by *extrusion*, a single aluminum bar can be formed then sliced into gears. Gears that have to sustain high loads with respect to their size are generally made of steel and are cut either *generating cutters* or *form cutters*. In form cutting, the tooth space takes the exact shape of the cutter. Whereas in generating, the tool has a shape different than the tooth profile desired and it is moved relative to the blank gear in a way as to obtain the correct tooth shape.

Gear teeth can be machined by *milling*, *shaping*, or *hobbing.* They can be finished by *shaving*, *burnishing*, *grinding*, or *lapping*.

6.1 Milling

Gear teeth may be cut with a form milling cutter shaped to conform to the tooth space. With this method it is theoretically necessary to use a different cutter for each gear, because a gear having *n* teeth will have a different-shaped tooth space from one having *n+1* teeth. Actually, the change in space is not too great, and it has been found that eight cutters may be used to cut with reasonable accuracy any gear in the range of 12 teeth to a rack. A separate set of cutters is required for each pitch for sure.

In Figure (6.1) can be seen the golden cutter gear rotating about its axis while the gray blank gear is in a fixed position. When each tooth space is completely cut, the blank gear is rotated about its own axis by an increment angle corresponding to a full tooth, also known as *angular pitch* θ_N:

$$\theta_N = \frac{p}{\rho_p} = \frac{2pP}{N} = \frac{2\pi}{N} \qquad \text{Equation 6.1}$$

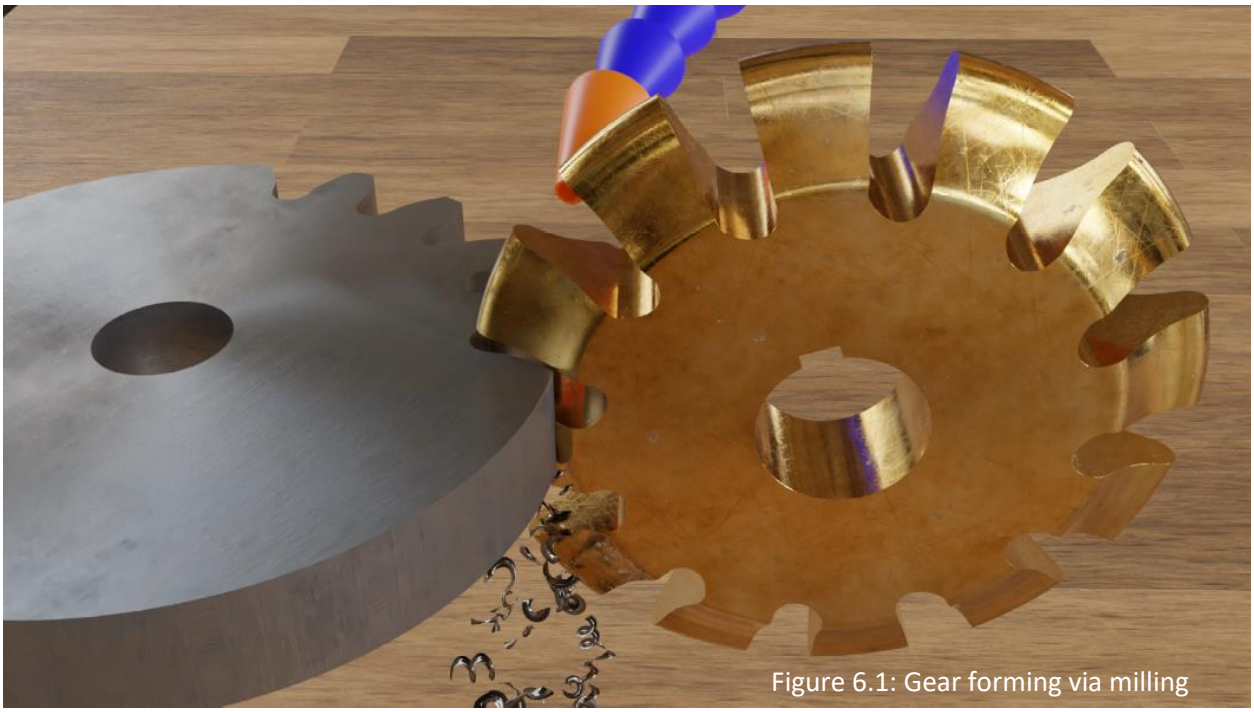

Figure 6.1: Gear forming via milling

6.2 Hobbing

The hob (golden tool in Figure 6.2) is a cutting tool that is shaped like a worm, and has a motion sequence like that of worm. The teeth have straight sides, as in a rack, but the hob axis must be turned through the lead angle in order to cut spur-gear teeth. The cross-sectional profile of the hob is actually identical to that of a rack. During one rotation of the hob, the gear moves forward by one tooth. In this respect, the pitch of the cutters corresponds exactly to the tooth pitch of the gear. Therefore, both the hob and the blank must be rotated at the proper angular-velocity ratio. When manufacturing a gear with *n* teeth, the rotational speed of the hob must be *n* times higher than the speed of the gear. The hob is fed slowly across the face of the blank until all the teeth have been cut.

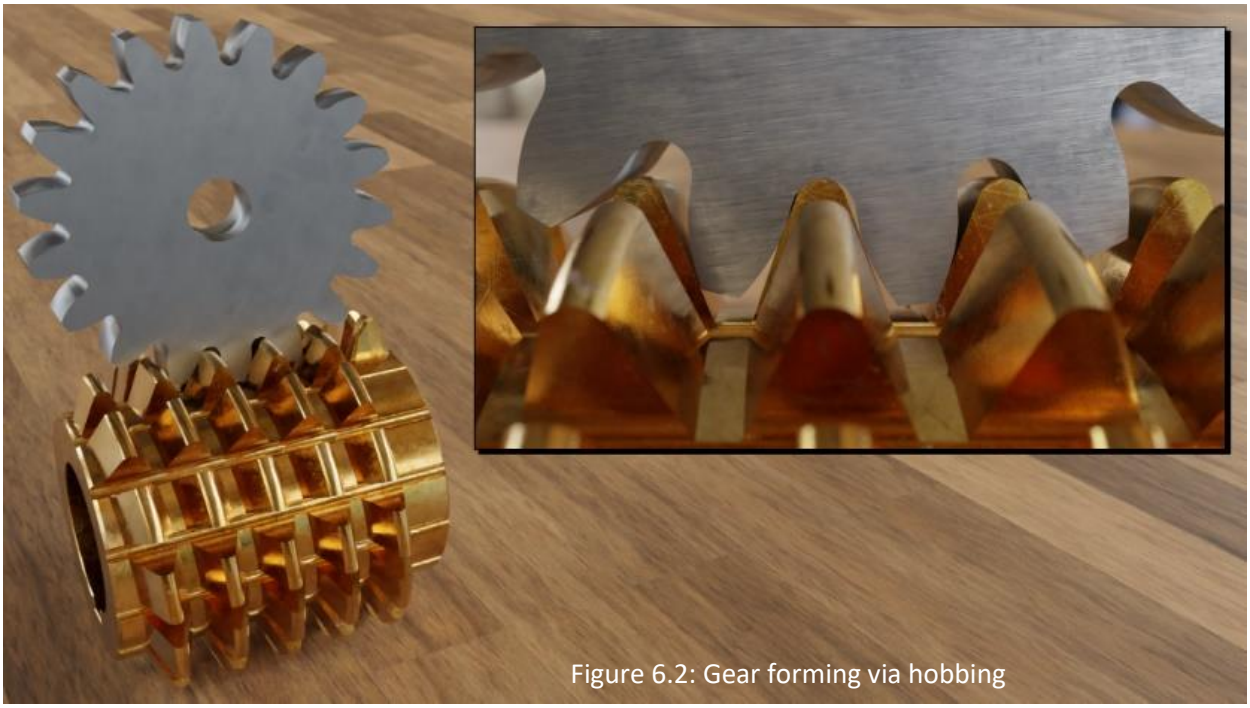

Figure 6.2: Gear forming via hobbing

Figure (6.3) is a schematic of the main parameters of the hob profile. The resemblance of the hob to a rack is quite apparent. The geometry mainly depends on the desired flank profile of the gear tooth. The tool flanks have an inclination angle against the vertical equal to the desired *pressure angle* α_0 (usually equal to 20^o). The *profile center line* corresponds to the pitch line of the gear with p_0 the circular pitch, and the maximum height of the fillet on the top of the hob teeth is equal to the clearance distance c.

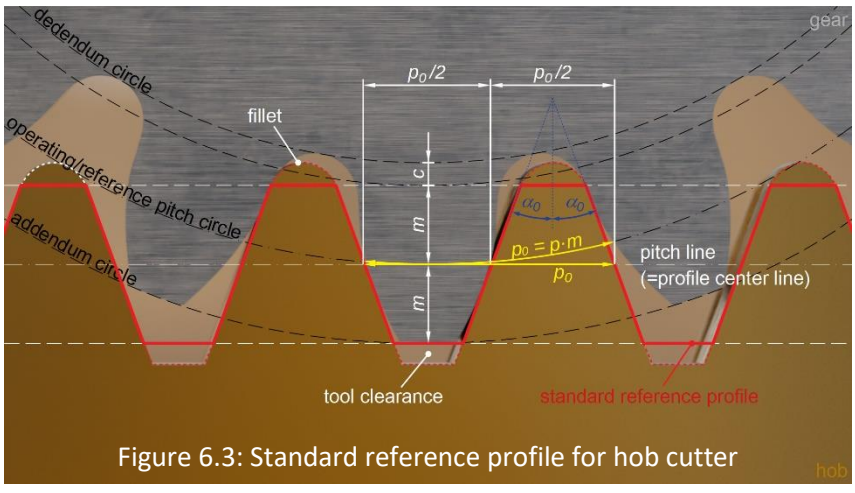

Figure 6.3: Standard reference profile for hob cutter

6.3 Shaping

Teeth may be generated with either a pinion cutter or a rack cutter. The pinion cutter reciprocates along an axis perpendicular to its plane and is slowly fed into the gear blank to the required depth. When the pitch circles are tangent, both the cutter and the blank rotate slightly after each cutting stroke. Since each tooth of the cutter is a cutting tool, the teeth are all cut after the blank has completed one rotation. The sides of an involute rack tooth are straight. For this reason, a rack generating tool provides an accurate method of cutting gear teeth. In operation, the cutter reciprocates and is first fed into the gear blank until the pitch circles are tangent. Then, after each cutting stroke, the gear blank and cutter roll slightly on their pitch circles. When the blank and cutter have rolled a distance equal to the circular pitch, the cutter is returned to the starting point, and the process is continued until all the teeth have been cut.

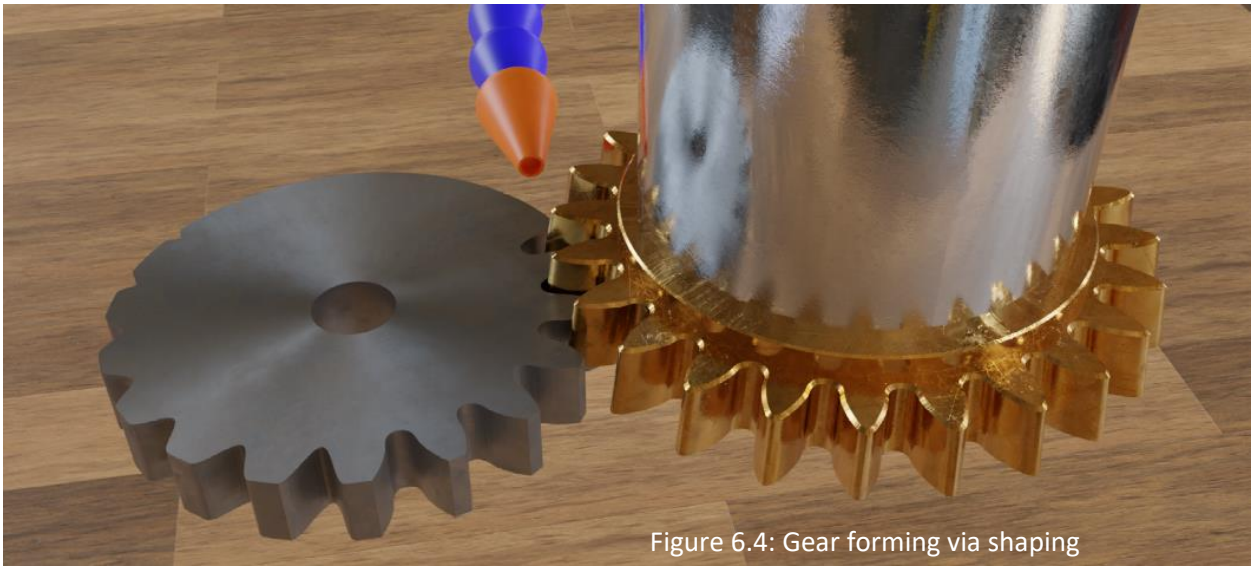

Figure 6.4: Gear forming via shaping

Figure (6.5) shows the relation between gear and rack dimensions. The perpendicular distance between the involutes for all gears with the same module always corresponds to the perpendicular distance between two adjacent flanks. This distance is referred to as *base pitch* p_b and corresponds to the distance between two contacting flanks in mesh with a mating gear (or rack).

In addition to that, Figure (6.5) shows that the *base pitch* p_b is directly related to the *circular pitch* p_0 by the standard pressure angle α_0 (Equation 6.1). It's worth noting that the *circular pitch* p_0 is identical for all gears with the same module (evidenced in equation 2.3), otherwise they cannot mesh properly. This is why the *circular pitch* p_0 of the rack is also equal to the *circular pitch* of the gears.

$$p_b = p_0 . cos\alpha_0 \qquad \text{Equation 6.1}$$

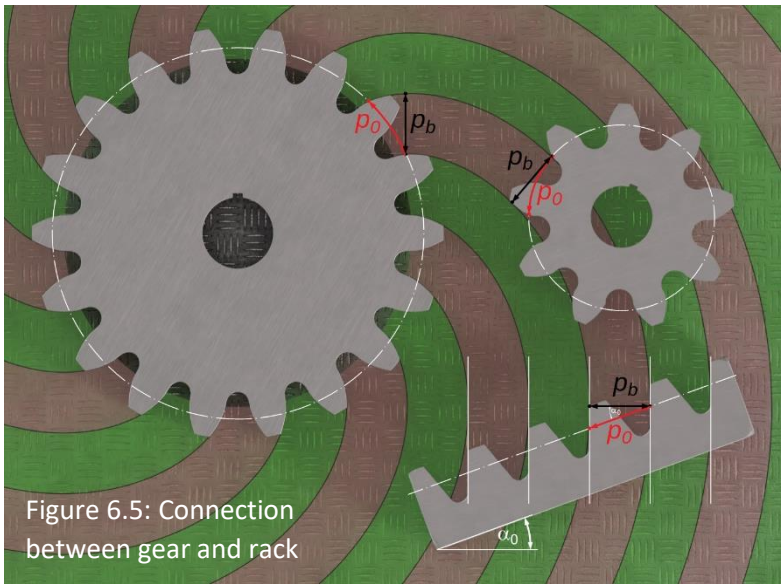

Figure 6.5: Connection between gear and rack

7. Contact Ratio

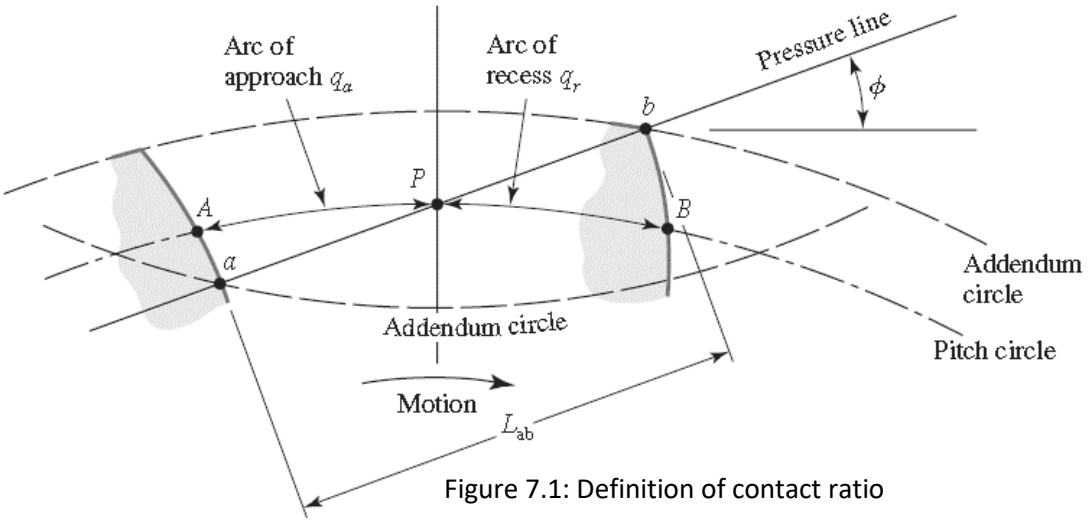

Figure 7.1: Definition of contact ratio

Figure (7.1) shows the action zone of meshed gear teeth. Point *a* represent the initial contact point. Point *b* represents the final contact point. Both points *a* and *b* are in fact the intersections between the addendum circles and the *pressure line*. Tooth profiles drawn through points *a* and *b* intersect the pitch circle at points *A* and *B,* respectively. The distance *AP* is known as the *arc of approach* q_a, and the distance *PB* is known as the *arc of recess* q_r. The sum of these arcs is known as the *arc of action* q_t. $(q_t = q_a + q_r)$

We define the term *contact ratio* m_c as:

$$m_c = \frac{q_t}{p} \qquad \text{Equation 7.1}$$

a number that indicates the average number of pairs of teeth in contact.

If $q_t = p$, then $m_c = 1$, and that means that one tooth and its space will occupy the entire arc *AC*. When one tooth enters in contact at *a*, the previous tooth has just ended contact at *b*. If q_t is slightly larger than p, that means that for short periods of time two teeth will be in contact, one in the vicinity of *a* and one in the vicinity of *b*. The *contact ratio* is also equal to the length of the path of contact divided by the base pitch:

$$m_c = \frac{L_{ab}}{p.cos\phi} \qquad \text{Equation 7.2}$$

where L_{ab} is the length of line ab, and the base pitch p_b is substituted by its equivalent expression from Equation (6.1).

Gears should not have a *contact ratio* no less than approximately 1.20, because mounting inaccuracies can reduce the *contact ratio* even further, which leads to more impact between teeth and by extension, more noise.

8. Tooth Systems

A *tooth system* is a standard that specifies the relationships involving addendum, dedendum, working depth, tooth thickness, and pressure angle. The standards were originally planned to attain interchangeability of gears of all tooth numbers, but of the same pressure angle and pitch.

Table (8.1) contains the latest standards most used for spur gears. The standardization was done by the American Gear Manufacturers Association (AGMA) and changes are made from time to time.

A 7.5^{o} pressure angle was once used for these but is now obsolete; the resulting gears had to be comparatively larger to avoid interference problems.

Tooth System	Pressure Angle ϕ, deg	Addendum a	Dedendum b
Full depth	20	$1/P_d$ or $1m$	$1.25/P_d$ or $1.25m$
			$1.35/P_d$ or $1.35m$
	$22\frac{1}{2}$	$1/P_d$ or $1m$	$1.25/P_d$ or $1.25m$
			$1.35/P_d$ or $1.35m$
	25	$1/P_d$ or $1m$	$1.25/P_d$ or $1.25m$
			$1.35/P_d$ or $1.35m$

Table 8.1: Standards and commonly used tooth systems for spur gears

Table (8.2) is particularly useful in selecting the pitch or module of a gear. Cutters are generally available for the sizes shown in this table.

Diametral Pitch	
Coarse	$2, 2\frac{1}{4}, 2\frac{1}{2}, 3, 4, 6, 8, 10, 12, 16$
Fine	20, 24, 32, 40, 48, 64, 80, 96, 120, 150, 200
Modules	
Preferred	1, 1.25, 1.5, 2, 2.5, 3, 4, 5, 6, 8, 10, 12, 16, 20, 25, 32, 40, 50
Next Choice	1.125, 1.375, 1.75, 2.25, 2.75, 3.5, 4.5, 5.5, 7, 9, 11, 14, 18, 22, 28, 36, 45

Table 8.2: Tooth sizes in general uses

In what follows is presented the shaping process by pinion cutter in its profile generation aspect for spur gears.

9. Coordinate Transformation for externally tangent spur gears

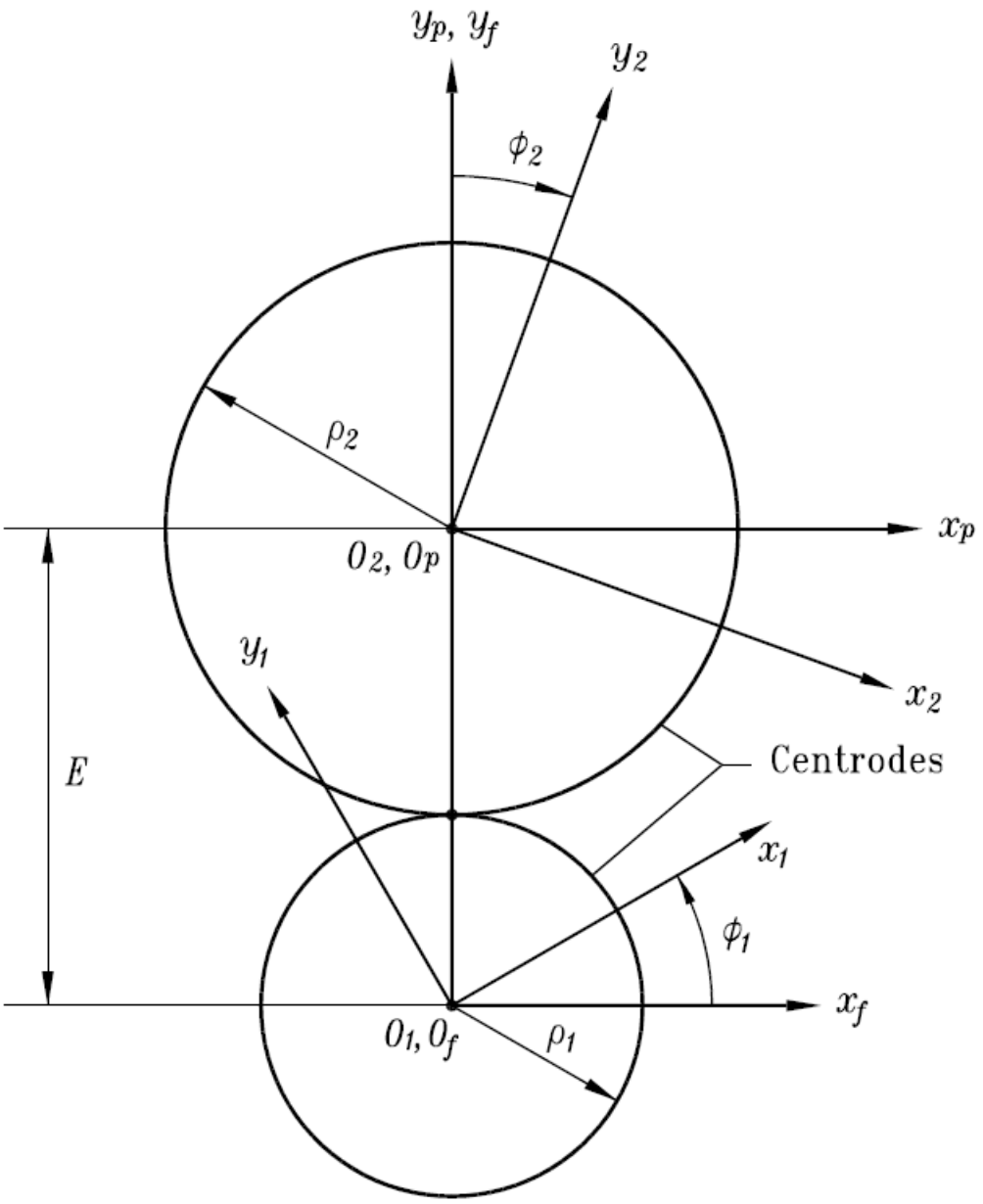

Figure 9.1: centrodes in rotational motions in opposite directions.

In figure (9.1) are shown 2 tangential centrodes with 4 coordinates systems:

- $S_1(O_1, x_1, y_1, z_1)$ is the primary coordinate system rigidly connected to rotating gear 1.
- $S_2(O_2, x_2, y_2, z_2)$ is the primary coordinate system rigidly connected to rotating gear 2.
- $S_f(O_f, x_f, y_f, z_f)$ is an auxiliary coordinate system rigidly connected to the gear housing.
- $S_p(O_p, x_p, y_p, z_p)$ is an auxiliary coordinate system rigidly connected to the gear housing.

ϕ_1 and ϕ_2 are related by equation (9.1):

$$\frac{\phi_1}{\phi_2} = \frac{\rho_2}{\rho_1} \qquad \text{Equation 9.1}$$

E is the shortest distance between the 2 axes of rotation. ($E = \rho_1 + \rho_2$)

To find the coordinates of points from centrode 2 to centrode 1, a coordinate transformation transition is required, and is based on the relation in the matrix equation (9.2):

$$r_1 = M_{12} r_2 = M_{1f} M_{fp} M_{p2} r_2 \qquad \text{Equation 9.2}$$

where M_{1f} and M_{p2} are rotational matrices and M_{fp} is a translational matrix.

$$r_2 = \begin{bmatrix} x_2 \\ y_2 \\ z_2 \\ 1 \end{bmatrix}, \qquad M_{p2} = \begin{bmatrix} cos\phi_2 & sin\phi_2 & 0 & 0 \\ -sin\phi_2 & cos\phi_2 & 0 & 0 \\ 0 & 0 & 1 & 0 \\ 0 & 0 & 0 & 1 \end{bmatrix}$$

$$r_1 = \begin{bmatrix} x_1 \\ y_1 \\ z_1 \\ 1 \end{bmatrix}, \qquad M_{1f} = \begin{bmatrix} cos\phi_1 & sin\phi_1 & 0 & 0 \\ -sin\phi_1 & cos\phi_1 & 0 & 0 \\ 0 & 0 & 1 & 0 \\ 0 & 0 & 0 & 1 \end{bmatrix}$$

$$M_{fp} = \begin{bmatrix} 1 & 0 & 0 & 0 \\ 0 & 1 & 0 & E \\ 0 & 0 & 1 & 0 \\ 0 & 0 & 0 & 1 \end{bmatrix}.$$

It is assumed that positive angles are clockwise.

Equation (9.2) gives

$$M_{12} = \begin{bmatrix} \cos(\phi_1 + \phi_2) & \sin(\phi_1 + \phi_2) & 0 & E\, sin\phi_1 \\ -\sin(\phi_1 + \phi_2) & \cos(\phi_1 + \phi_2) & 0 & E\, cos\phi_1 \\ 0 & 0 & 1 & 0 \\ 0 & 0 & 0 & 1 \end{bmatrix}$$

The inverse transformation can be done using matrix $M_{21} = M_{12}^{-1}$ in equation (9.3):

$$r_2 = M_{21} r_1 \qquad \text{Equation 9.3}$$

where

$$M_{21} = \begin{bmatrix} \cos(\phi_1 + \phi_2) & -\sin(\phi_1 + \phi_2) & 0 & E\, sin\phi_2 \\ \sin(\phi_1 + \phi_2) & \cos(\phi_1 + \phi_2) & 0 & -E\, cos\phi_2 \\ 0 & 0 & 1 & 0 \\ 0 & 0 & 0 & 1 \end{bmatrix}$$

10. Applications for external spur gears

10.1 Application to a generic shape

In the following is discussed the generation of the gear tooth profile by a generic trapezoidal shape via 2 tangent circles rotating without slipping.

The generic trapezoidal tooth used is shown in figure (10.1). By setting the coordinates of the trapeze in coordinate system S_2 and pre-multiplying them with the transformation matrix M_{12} according to equation (9.2), coordinate in system S_1 are found.

Running a loop continuously varying ϕ angles, the motion of the generic tooth can be generated and visualized by the successive positions taken by the 6 points as can be seen in figure (10.2).

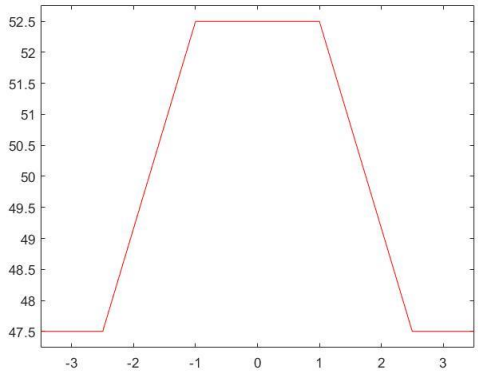

Figure 10.1: generic tooth shape

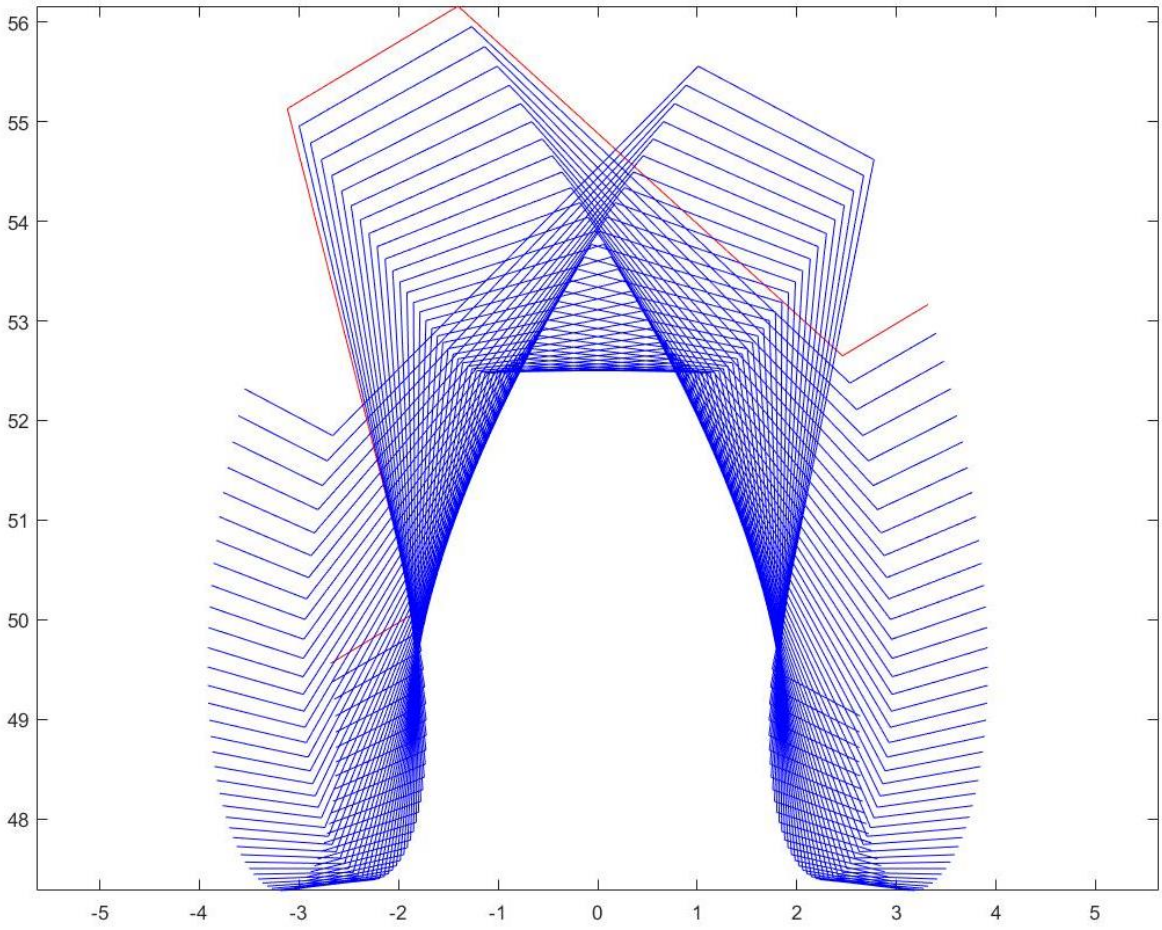

Figure 10.2: generated tooth

Both centrodes have a radius of 50 units in the previous simulation: $(E = R_1 + R_2 = 100)$

10.2 Refined application

10.2.1 Data given

➢ The shaper cutter data is as follows:

- Tooth profile is shown in Figure (10.3)
- Number of teeth: $N = 17$
- Module: $m = 3$
- Pressure angle: $\alpha = 20^o$
- Radius: $R_1 = \frac{mN}{2} = 25.5$ Equation 10.1

➢ Target dimension for the blank gear:

- $R_2 = R_1 = 25.5$

Both the shaper and the work gears are assumed to have identical radii equal to 25.5 according to the previous equation and equal number of teeth ($N = 17$).

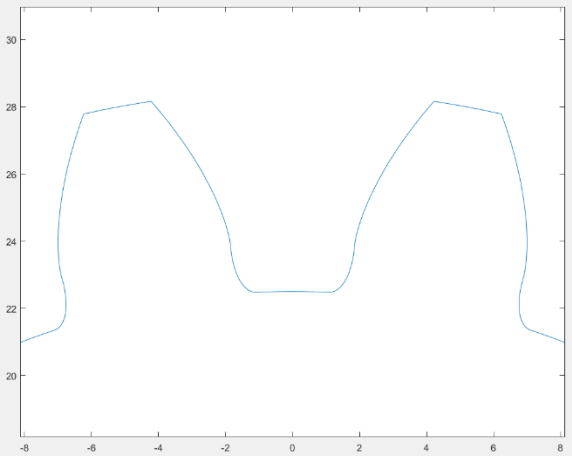

Figure 10.3: 2-teeth section of the shaper gear

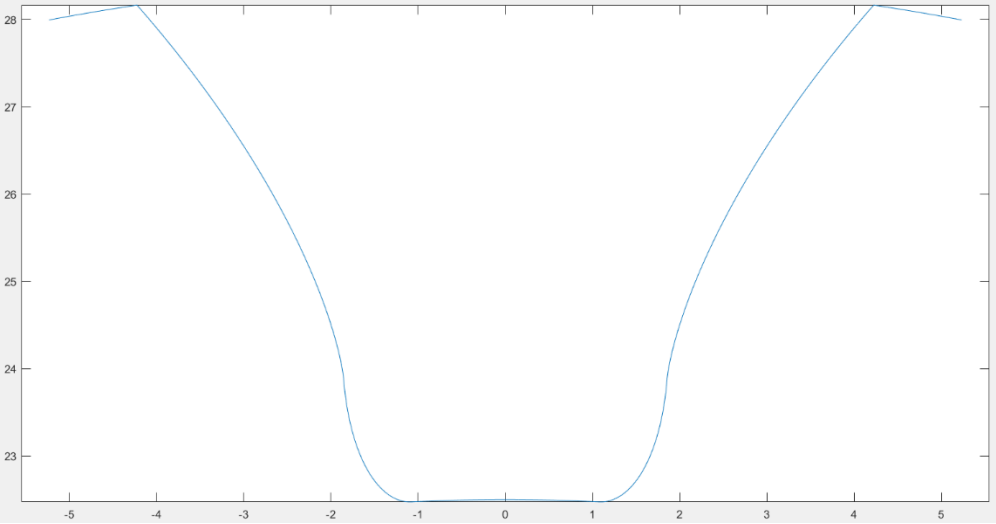

Figure 10.4: Shaper gear cutter vane profile

In the following, the shaper gear cutter vane profile shown in figure (10.4) will be used in order to generate a tooth shape in the work gear, instead of using the tooth profile to generate a vane shape.

10.2.2 Results

The vane profile data is given as x, y coordinates in the $S_2(O_2, x_2, y_2, z_2)$ coordinate system represented in figure (9.1).

Using equation (9.2) and matrix M_{12} for continuously incremented ϕ angles (always in relation according to equation (9.1)), it is possible to find the trajectory of the vane profile with respect to the $S_1(O_1, x_1, y_1, z_1)$ coordinate system.

By plotting those consecutive positions, the tooth profile on the work gear is generated as is shown is figure (10.5).

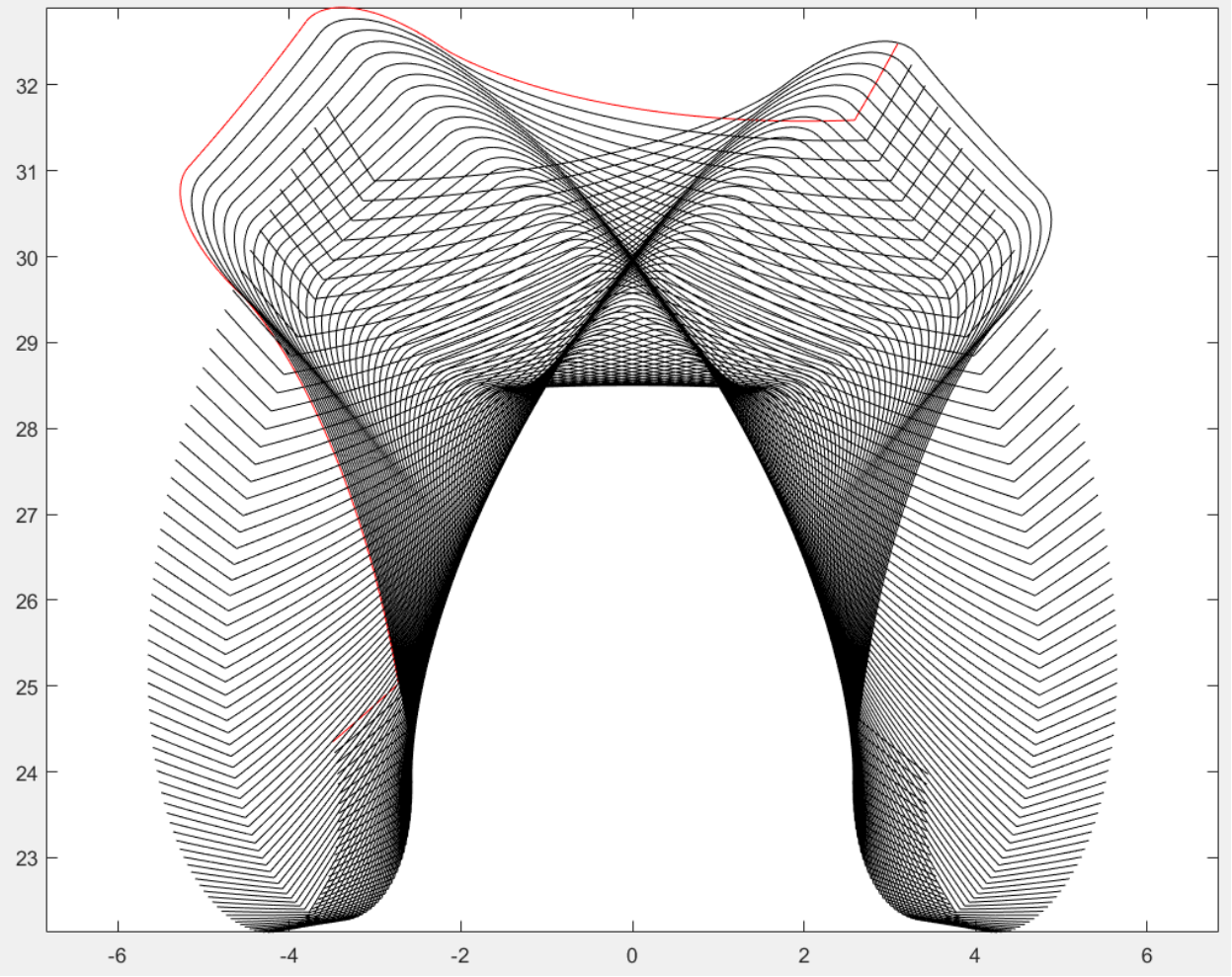

Figure 10.5: Generated tooth profile on the work gear

It is worth noting that a shaper cutter with involute profiles create teeth with identical flank profile to the cutter.

11. Coordinate transformation for internally tangent spur gears

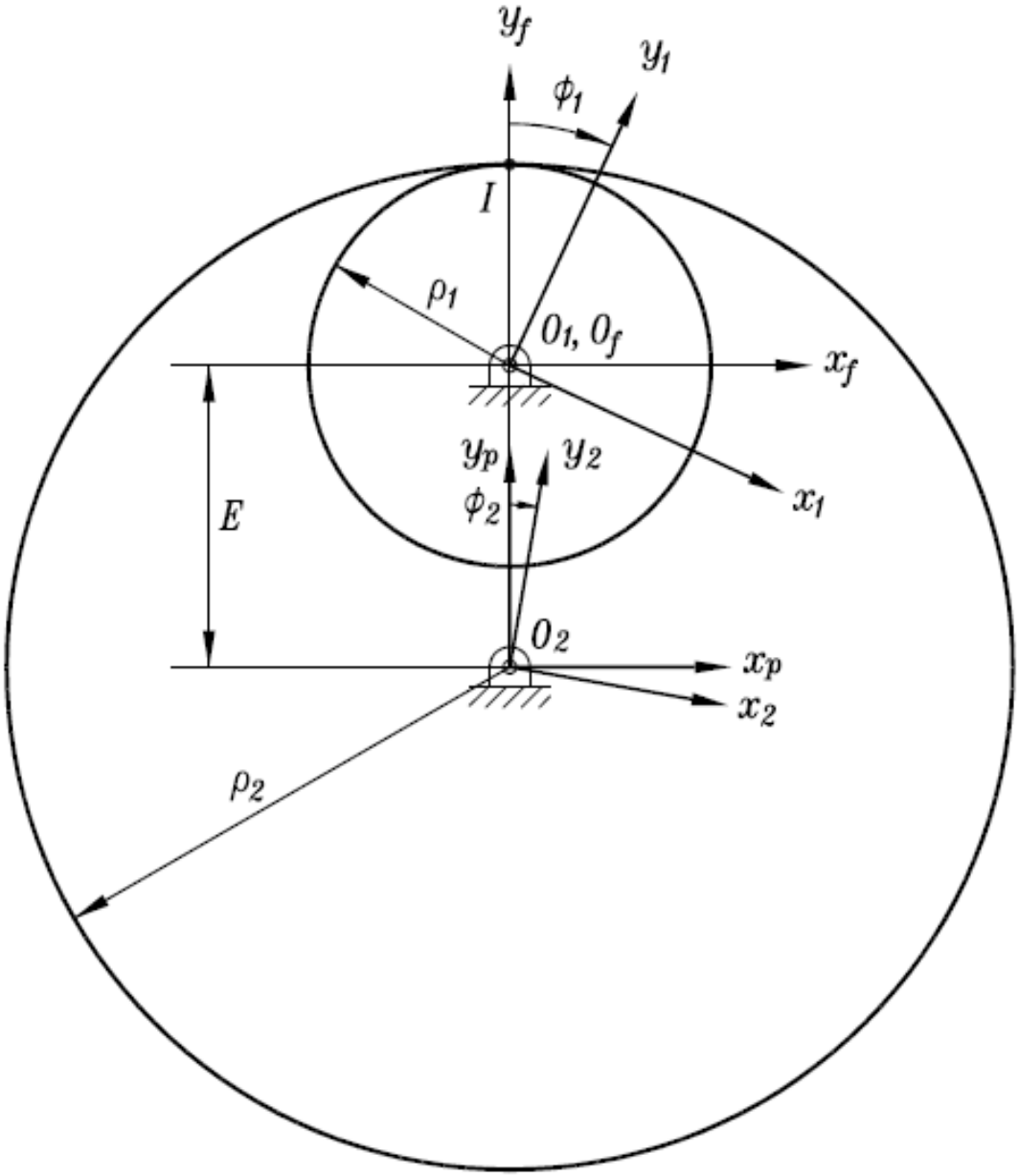

Figure 11.1: centrodes in rotational motions of the same direction

In Figure (11.1) are shown 2 tangential centrodes with 4 coordinates systems:

- $S_1(O_1, x_1, y_1, z_1)$ is the primary coordinate system rigidly connected to rotating gear 1.
- $S_2(O_2, x_2, y_2, z_2)$ is the primary coordinate system rigidly connected to rotating gear 2.
- $S_f(O_f, x_f, y_f, z_f)$ is an auxiliary coordinate system rigidly connected to the gear housing.
- $S_p(O_p, x_p, y_p, z_p)$ is an auxiliary coordinate system rigidly connected to the gear housing.

Centrode 2 is assumed to be the external centrode ($\rho_2 > \rho_1$).

ϕ_1 and ϕ_2 are related by equation (11.1):

$$\frac{\phi_1}{\phi_2} = \frac{\rho_2}{\rho_1} \qquad \text{Equation 11.1}$$

E is the shortest distance between the 2 axes of rotation. ($E = \rho_2 - \rho_1$)

To find the coordinates of points from centrode 2 to centrode 1, a coordinate transformation transition is required, and is based on the relation in the matrix equation (11.2):

$$r_1 = M_{12} r_2 = M_{1f} M_{fp} M_{p2} r_2 \qquad \text{Equation 11.2}$$

where M_{1f} and M_{p2} are rotational matrices and M_{fp} is a translational matrix.

$$r_2 = \begin{bmatrix} x_2 \\ y_2 \\ z_2 \\ 1 \end{bmatrix}, \qquad M_{p2} = \begin{bmatrix} cos\phi_2 & sin\phi_2 & 0 & 0 \\ -sin\phi_2 & cos\phi_2 & 0 & 0 \\ 0 & 0 & 1 & 0 \\ 0 & 0 & 0 & 1 \end{bmatrix}$$

$$r_1 = \begin{bmatrix} x_1 \\ y_1 \\ z_1 \\ 1 \end{bmatrix}, \qquad M_{1f} = \begin{bmatrix} cos\phi_1 & -sin\phi_1 & 0 & 0 \\ sin\phi_1 & cos\phi_1 & 0 & 0 \\ 0 & 0 & 1 & 0 \\ 0 & 0 & 0 & 1 \end{bmatrix}$$

$$M_{fp} = \begin{bmatrix} 1 & 0 & 0 & 0 \\ 0 & 1 & 0 & -E \\ 0 & 0 & 1 & 0 \\ 0 & 0 & 0 & 1 \end{bmatrix}.$$

It is assumed that positive angles are clockwise.

Equation (11.2) gives

$$M_{12} = \begin{bmatrix} \cos(\phi_1 - \phi_2) & -\sin(\phi_1 - \phi_2) & 0 & E\ sin\phi_1 \\ \sin(\phi_1 - \phi_2) & \cos(\phi_1 - \phi_2) & 0 & -E\ cos\phi_1 \\ 0 & 0 & 1 & 0 \\ 0 & 0 & 0 & 1 \end{bmatrix}$$

The inverse transformation can be done using matrix $M_{21} = M_{12}^{-1}$ in equation (11.3):

$$r_2 = M_{21} r_1 \qquad \text{Equation 11.3}$$

where

$$M_{21} = \begin{bmatrix} \cos(\phi_1 - \phi_2) & \sin(\phi_1 - \phi_2) & 0 & -E\ sin\phi_2 \\ -\sin(\phi_1 - \phi_2) & \cos(\phi_1 - \phi_2) & 0 & E\ cos\phi_2 \\ 0 & 0 & 1 & 0 \\ 0 & 0 & 0 & 1 \end{bmatrix}$$

12. Application for internal spur gears

12.1 Data given

➢ The shaper cutter data is as follows:

- Tooth profile is shown in Figure (12.1)
- Number of teeth: $N_1 = 17$
- Module: $m = 3$
- Pressure angle: $\alpha = 20^o$
- Addendum: $a_1 = 1.3m$
- Dedendum: $b_1 = 1m$
- Radius: $R_1 = \frac{mN_1}{2} = 25.5$

➢ Target dimensions for the blank gear:

- Radius $R_2 = 8R_1 = 204$
- Number of teeth $N_2 = 8N_1 = 136$
- Addendum $a_2 = 1m$
- Dedendum $b_2 = 1.25m$

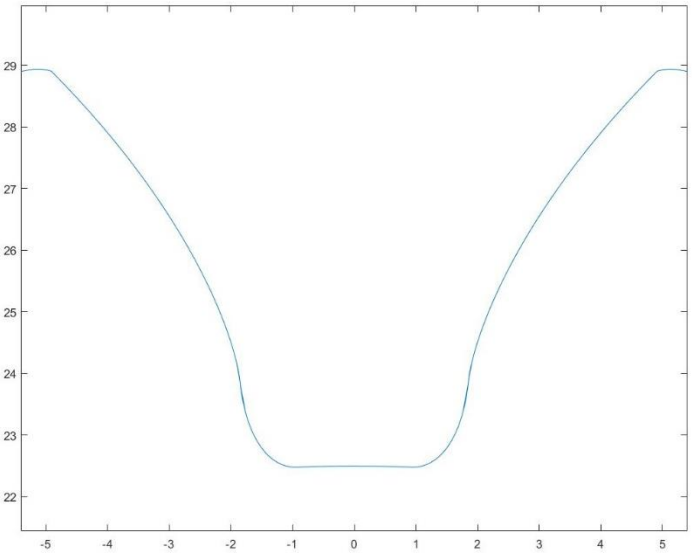

Figure 12.1: Shaper cutter gear vane profile

Addendum and Dedendum targets are selected in accord with tooth system standards from Table (8.1).

12.2 Results

The vane profile data is given as x, y coordinates in the $S_1(O_1, x_1, y_1, z_1)$ coordinate system represented in figure (11.1).

Using equation (11.3) and matrix M_{21} for continuously incremented ϕ angles (always in relation according to equation (11.1)), it is possible to find the trajectory of the vane profile with respect to the $S_1(O_1, x_1, y_1, z_1)$ coordinate system.

By plotting those consecutive positions, the tooth profile on the work gear is generated as is shown is Figure (12.2). It is noticeable that the generated tooth profile does not meet the targeted dimensions of addendum and dedendum.

Given that the inequality ($a_2 + b_2 < a_1 + b_1$) is verified, the issue can easily be solved by changing E, the distance between the centers of rotation of the cutter and blank gears according to equation (12.1)

$$E = R_2 - R_1 - offset \qquad \text{Equation 12.1}$$

with: $offset = a_1 - b_2$

Thus $E = R_2 - R_1 - a_1 + b_2$

After correction, results are shown in Figure (12.3). The blank gear dedendum matches the requirement, but the addendum is slightly larger than wanted (area situated beneath the tooth envelope and above the yellow addendum circle). This, however, is not an issue. That additional area can be easily removed via a separate machining process or even by sizing the inner diameter of the blank gear accordingly before cutting the blank gear. It is common with shaper cutter that the dedendum of the tool be greater than the addendum of the blank gear to be cut. Addendum is set from the blank gear itself.

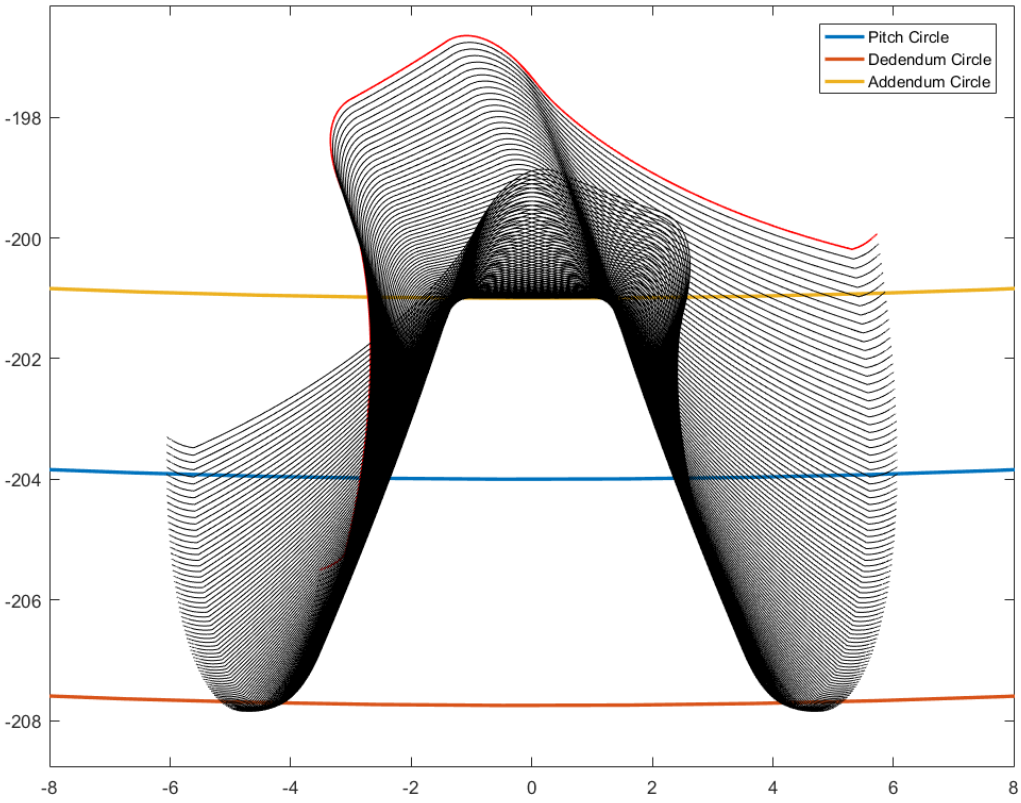

Figure 12.2: Generated tooth shape pre-correction

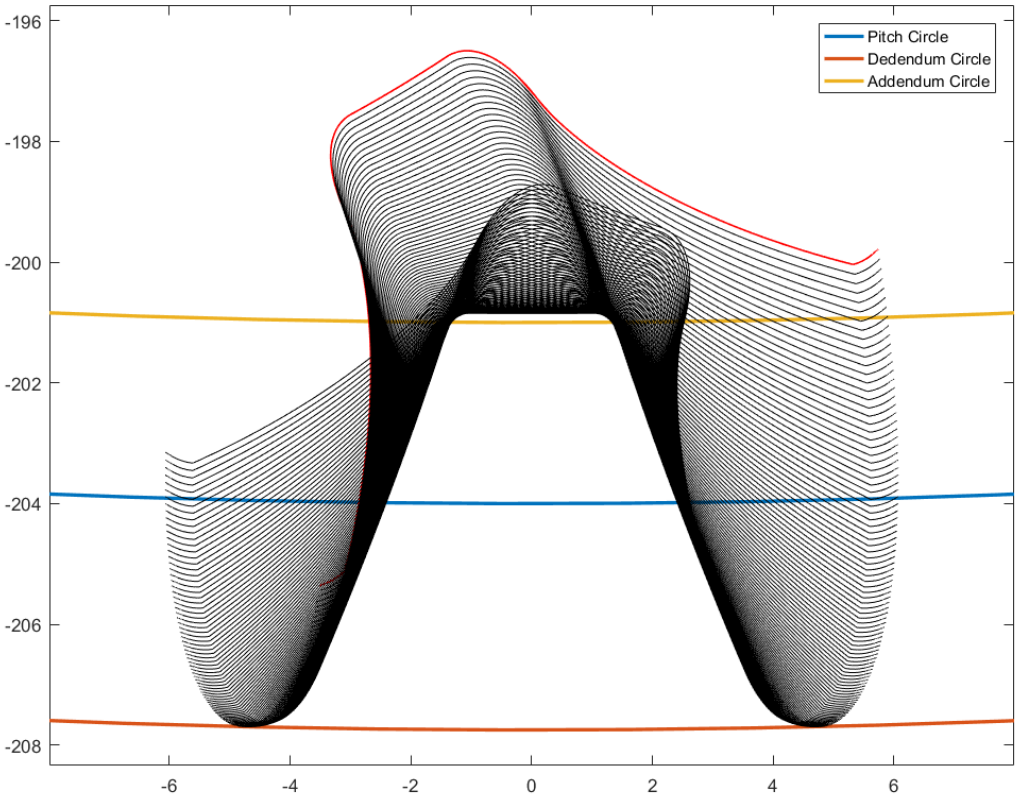

Figure 12.3: Generated tooth shape post-correction

13. Involute helical gears with parallel axes

Helical gears can be used to transmit motion between parallel shafts. The helix angle should be identical on both gears, but one gear must have a right-hand helix and the other a left-hand helix in order for them to mesh properly. Consequently, the shape of the tooth is an involute helicoid, shown in Figure (13.1).

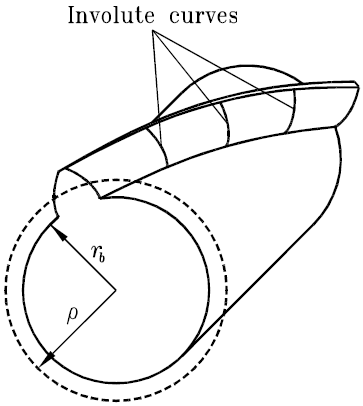

Figure 13.1: Helical gear tooth

Conversely to spur gears, whose contact is a line extending all the way across the face of the tooth, the initial contact of helical-gear teeth is a point that extends into a line as the line comes into more engagement. In spur gears the line of contact is parallel to the axis of rotation (Figure 13.2b), while in helical gears the line is diagonal across the face of the tooth (Figure 13.2a). This progressive engagement ensures a smooth load transfer from one tooth to another which allows helical gears to transmit heavy loads at high speeds.

Due to this different nature of contact in helical gears, the contact ratio is of little significance, rather it's the contact area, proportional to the face width of the gear, that is significant.

Helical gears subject the shaft bearings to radial and thrust loads. When thrust loads exceed allowable values, it is advisable to mount a double helical gear (herringbone) that is equivalent to two helical gears of opposite orientation mounted side by side on the same shaft. The thrust load cancels out because each pair of gears develop a thrust load opposite to the other.

When mounting more than a single helical gear on the same shaft, the hand of the gears should always be selected in a way to reduce the total thrust load generated as much as possible.

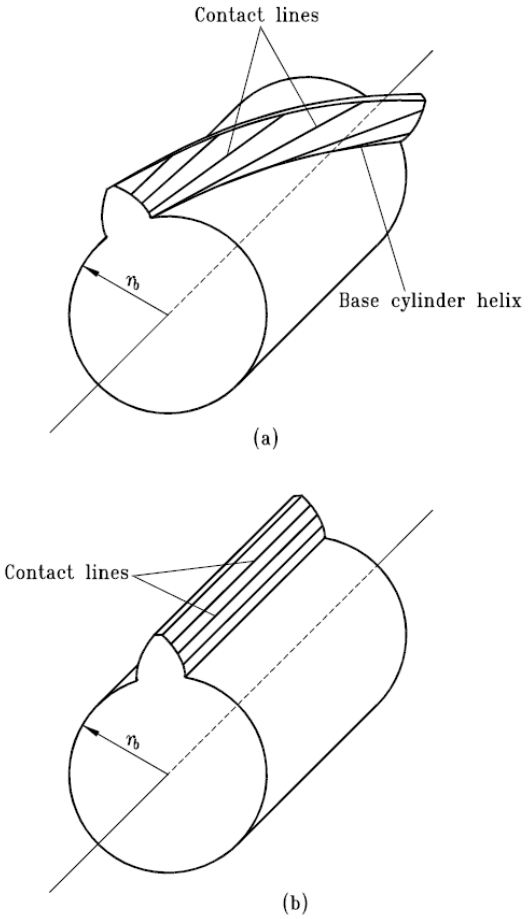

Figure 13.2: Contact lines on tooth surfaces of a helical gear (a) and a spur gear (b)

Figure (13.3) shows a top view of a helical rack, which will be used to define some parameters related to helical gears. Lines *ab* and *cd* are the centerlines of two adjacent helical teeth taken from the same pitch plane. The angle ψ is the *helix angle*. The distance *ac* is the *transverse circular pitch* p_t in the plane of rotation (usually referred to as the *circular pitch*). The distance *ae* is the *normal circular pitch* p_n and is related to the *transverse* circular pitch by

$$p_n = p_t cos\psi \qquad \text{Equation 13.1}$$

The distance *ad* is the *axial pitch* p_x and is related to previous parameters by

$$p_x = \frac{p_t}{tan\psi}$$ Equation 13.2

Since $p_n P_n = \pi$, the *normal diametral pitch* is presented by

$$P_n = \frac{P_t}{cos\psi}$$ Equation 13.3

The pressure angle ϕ_n in the normal direction is different from the pressure angle ϕ_t in the direction of rotation, because of the angularity of the teeth. These angles are related by

$$cos\psi = \frac{tan\phi_n}{tan\phi_t}$$ Equation 13.4

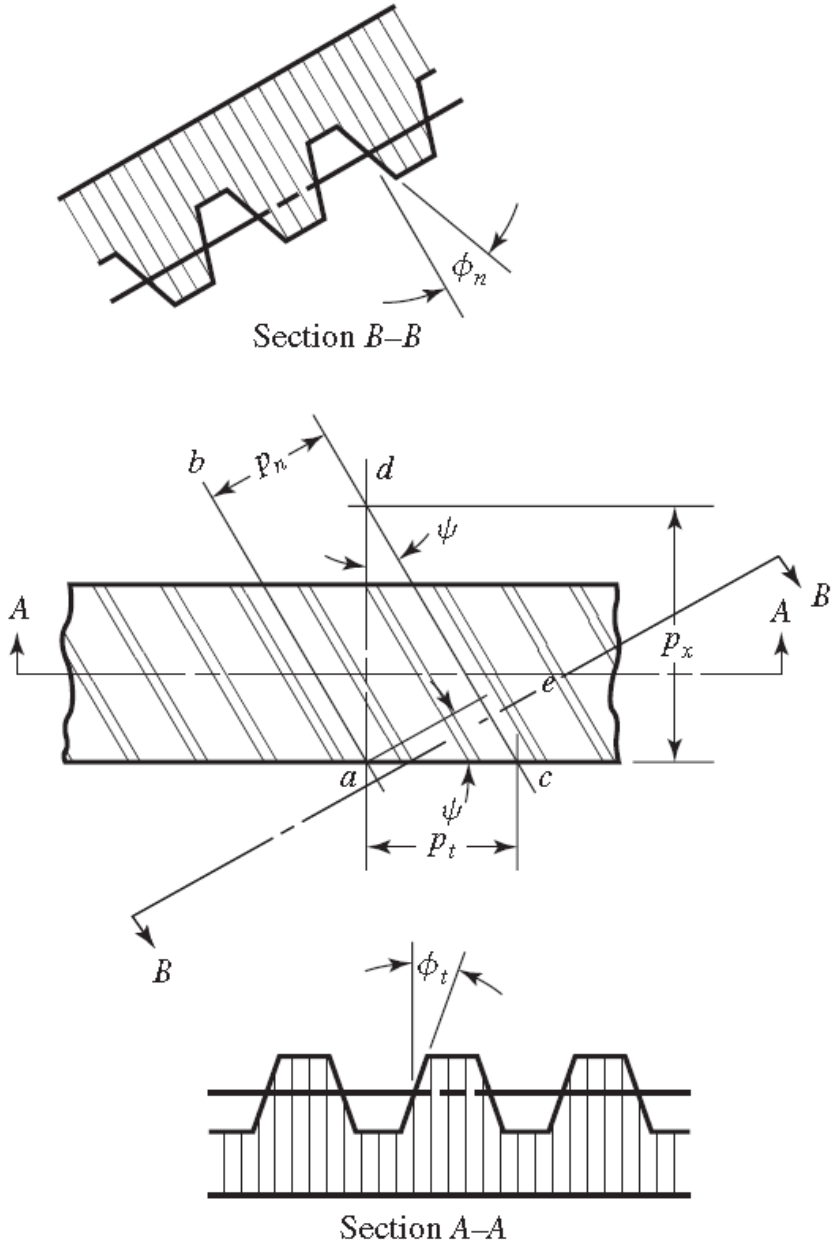

Figure 13.3: Nomenclature of helical gears

13.1 Design procedure

The design parameters of the normal section of the helical rack cutter are standardized. A standard helical gear is generated when the middle line of Section *A-A* in Figure (13.3) lies in the plane that is tangent to the gear pitch cylinder. The input data for computation of the design parameters of a standard helical gear are:

- *Normal pressure angle* ϕ_n
- *Normal diametral pitch* P_n
- *Helix angle* ψ
- *Number of teeth* N
- *Addendum* $a = 1/P_n$
- *Dedendum* $b = 1.25/P_n$

The procedure is as follows:

- *Lead angle on the pitch cylinder* λ_p (complement of the helix angle)*:*

$$\lambda_p = \frac{\pi}{2} - \psi \qquad \text{Equation 13.5}$$

- *Tangential pressure angle* ϕ_t*:*

$$tan\phi_t = \frac{tan\phi_n}{cos\psi} \qquad \text{Equation 13.6}$$

- *Tangential circular pitch* p_t*:*

$$p_t = \frac{p_n}{sin\lambda_p} = \frac{p_n}{cos\psi} \qquad \text{Equation 13.7}$$

- *Tangential diametral pitch* P_t*:*

$$P_t = P_n sin\lambda_p = P_n cos\psi \qquad \text{Equation 13.8}$$

- *Radius* r_p *of the pitch cylinder:*

$$r_p = \frac{N}{2P_t} = \frac{N}{2P_n sin\lambda_p} = \frac{N}{2P_n cos\psi} \qquad \text{Equation 13.9}$$

- *Radius* r_b *of the base cylinder:*

$$r_b = r_p cos\phi_t = \frac{N cos\phi_t}{2P_n cos\psi} \qquad \text{Equation 13.10}$$

- *Lead angle* λ_b *on the base cylinder:*

$$tan\lambda_b = \frac{p}{r_b} = \frac{r_p tan\lambda_p}{r_b} \qquad \text{Equation 13.11}$$

Alternative equation for λ_b:

$$cos\lambda_b = cos\lambda_p cos\phi_n \qquad \text{Equation 13.12}$$

- *Addendum radius of the cylinder:*

$$r_a = r_p + a = \frac{N + 2sin\lambda_p}{2P_n sin\lambda_p} = \frac{N + 2cos\psi}{2P_n cos\psi} \qquad \text{Equation 13.13}$$

- *Dedendum radius of the cylinder:*

$$r_d = r_p - b = \frac{N - 2.5sin\lambda_p}{2P_n sin\lambda_p} = \frac{N - 2.5cos\psi}{2P_n cos\psi} \qquad \text{Equation 13.14}$$

- *Tooth thickness and Space width on the pitch circle:*

$$s_t = w_t = \frac{p_t}{2} = \frac{p_n}{2sin\lambda_p} = \frac{\pi}{2P_n sin\lambda_p} = \frac{\pi}{2P_n cos\psi} \qquad \text{Equation 13.15}$$

13.2 Virtual number of teeth

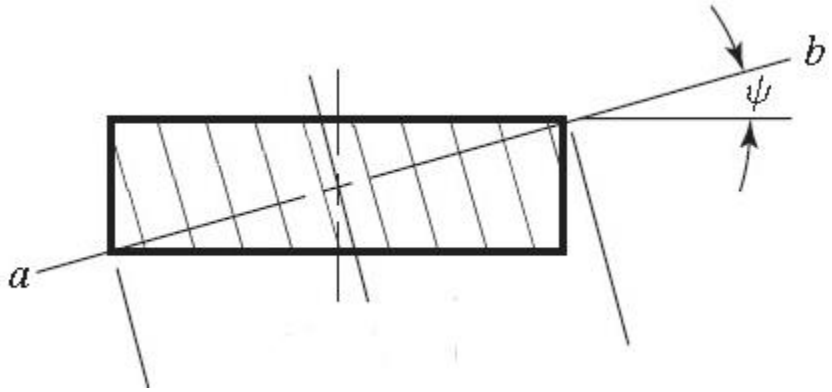

Figure 13.4: A cylinder cut by an oblique plane

Figure (13.4) shows a plane *ab* obliquely cutting a cylinder at an angle ψ. Plane *ab* cuts an ellipse through the cylinder. The shape of the tooth in the normal plane is nearly the same as the shape of a spur gear tooth having a pitch radius equal to radius of curvature R_e of the ellipse.

$$R_e = \frac{d}{2\cos^2\psi} \qquad \text{Equation 13.16}$$

For the condition of $\psi = 0$, the radius of curvature is $R_e = d/2$. If the angle ψ is increased from 0 to 90 degrees, R_e goes from a value of $d/2$ and tends to ∞.

The radius R_e is the apparent pitch radius viewed in the direction of the tooth elements. A gear having the same pitch p_n with a radius equal to R_e will have a greater number of teeth, due to the larger radius. In helical gear terminology, it's referred to as the *virtual number of teeth* N'.

$$N' = \frac{2R_e}{m_n} = \frac{d}{m_n\cos^2\psi} \qquad \text{Equation 13.17}$$

By substituting $m_n = m.cos\psi$, and $d = N.m$, we get

$$N' = \frac{N}{cos^3\psi} \qquad \text{Equation 13.18}$$

The *virtual number of teeth* is useful for design considerations for strength, and the apparently larger radius of curvature translates into the possibility of having fewer teeth per gear.

14. Coordinate transformation for externally tangent gears

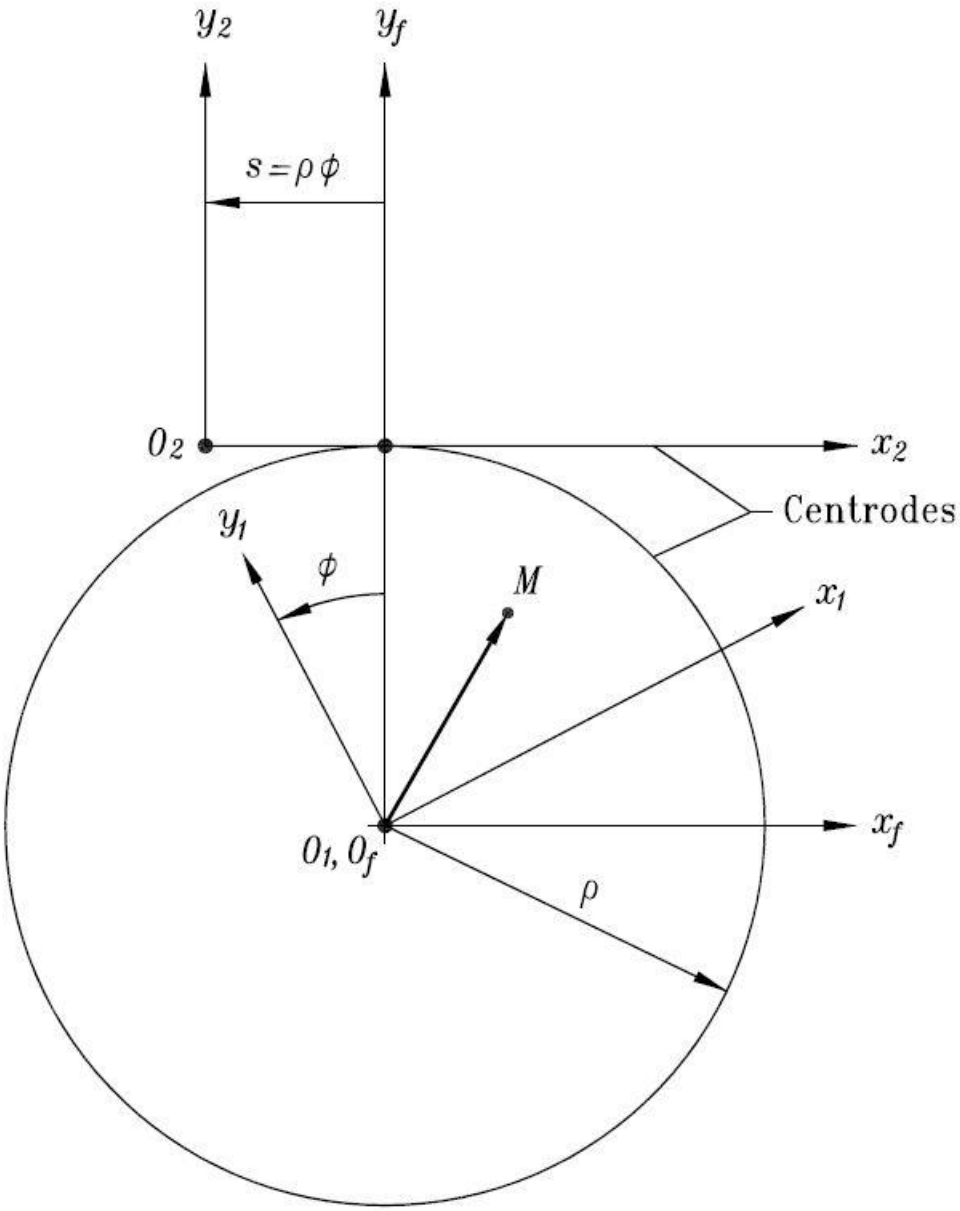

Figure 14.1: Centrodes in translation-rotation motions

In Figure (14.1) are shown 2 tangential centrodes with 3 coordinates systems:

- $S_1(O_1, x_1, y_1, z_1)$ is the primary coordinate system rigidly connected to the rotating gear.
- $S_2(O_2, x_2, y_2, z_2)$ is the primary coordinate system rigidly connected to the translating rack.
- $S_f(O_f, x_f, y_f, z_f)$ is an auxiliary coordinate system rigidly connected to the gear housing.

Translation s and rotation ϕ are related by equation (14.1)

$$s = \rho\phi \qquad \text{Equation 14.1}$$

To find the coordinates of points from centrode 1 to centrode 2, a coordinate transformation transition is required, and is based on the relation in the matrix equation (14.2):

$$r_1 = M_{12}r_2 = M_{1f}M_{f2}r_2 \qquad \text{Equation 14.2}$$

where M_{1f} is a rotational matrix and M_{f2} is a translational matrix.

$$r_1 = \begin{bmatrix} x_1 \\ y_1 \\ z_1 \\ 1 \end{bmatrix}, \qquad M_{1f} = \begin{bmatrix} cos\phi & sin\phi & 0 & 0 \\ -sin\phi & cos\phi & 0 & 0 \\ 0 & 0 & 1 & 0 \\ 0 & 0 & 0 & 1 \end{bmatrix},$$

$$r_2 = \begin{bmatrix} x_2 \\ y_2 \\ z_2 \\ 1 \end{bmatrix}, \qquad M_{f2} = \begin{bmatrix} 1 & 0 & 0 & -\rho\phi \\ 0 & 1 & 0 & \rho \\ 0 & 0 & 1 & 0 \\ 0 & 0 & 0 & 1 \end{bmatrix}.$$

It is assumed that positive angles are clockwise.

Equation (14.2) gives

$$M_{12} = \begin{bmatrix} cos\phi & sin\phi & 0 & \rho(sin\phi - \phi cos\phi) \\ -sin\phi & cos\phi & 0 & \rho(cos\phi + \phi sin\phi) \\ 0 & 0 & 1 & 0 \\ 0 & 0 & 0 & 1 \end{bmatrix}$$

The inverse transformation can be done using matrix $M_{21} = M_{12}^{-1}$ in equation (14.3):

$$r_2 = M_{21}r_1 \qquad \text{Equation 14.3}$$

where

$$M_{21} = \begin{bmatrix} cos\phi & -sin\phi & 0 & \rho\phi \\ sin\phi & cos\phi & 0 & -\rho \\ 0 & 0 & 1 & 0 \\ 0 & 0 & 0 & 1 \end{bmatrix}$$

15. Application for parallel helical gears

15.1 Data given

The cutter rack is similar to the one shown in Figure (13.3) with the following input parameters:

- *Normal pressure angle* $\phi_n = 20^o$
- *Module* $m = 3$ *Circular pitch* $p = \pi m = 3\pi$
- *Helix angle* $\psi = 30^o$ *Tangential pressure angle* $\phi_t = \arctan\left(\frac{tan\phi_n}{cos\psi}\right)$
- *Number of teeth* $N = 17$
- *Addendum* $a = 1m = 3$
- *Dedendum* $b = 1.25m = 3.75$
- *Rack thickness* $t = 50$

A tangential tooth profile of the rack with the aforementioned parameters is shown in Figure (15.1) and the coordinates of its six vertices (A, B, C, D, E and F) can be defined the following RackProfile Matrices:

$$RackProfile1 = \begin{bmatrix} 0 & \frac{p}{4} - b.tan\phi_t & \frac{p}{4} + a.tan\phi_t & \frac{3p}{4} - a.tan\phi_t & \frac{3p}{4} + b.tan\phi_t & p \\ -b & -b & a & a & -b & -b \\ \frac{t}{2} & \frac{t}{2} & \frac{t}{2} & \frac{t}{2} & \frac{t}{2} & \frac{t}{2} \end{bmatrix}$$

$$RackProfile2 = RackPorfile1 - \begin{bmatrix} t.tan\psi \\ 0 \\ \frac{t}{2} \end{bmatrix}$$

A 3D representation of the rack vane is shown in Figure (15.2).

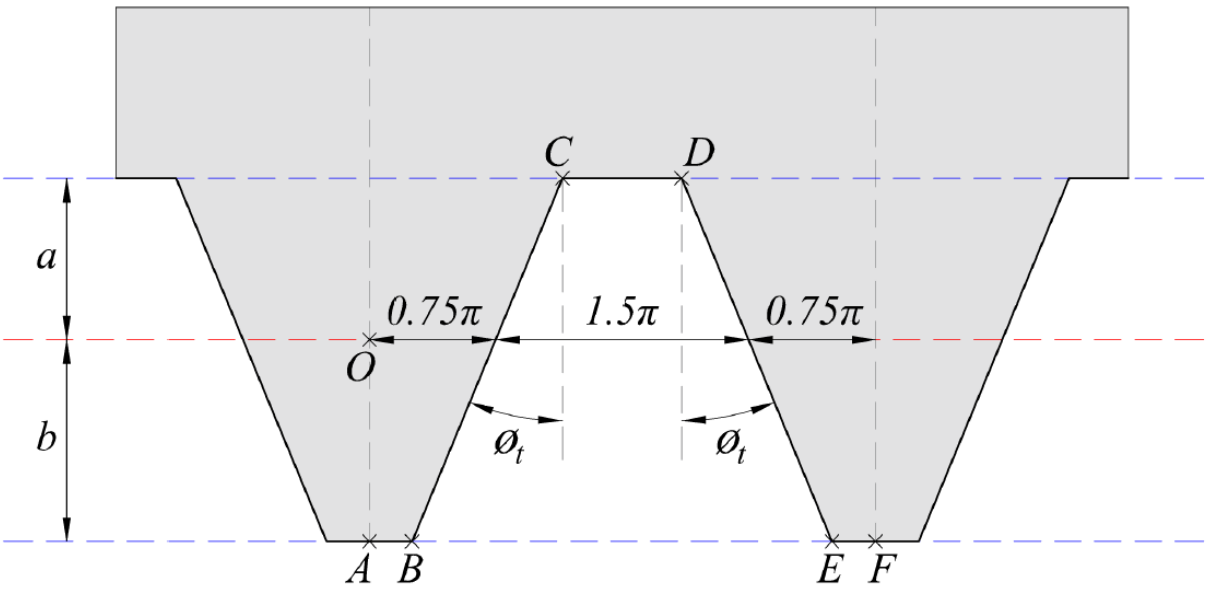

Figure 15.1: Rack tangential tooth profile

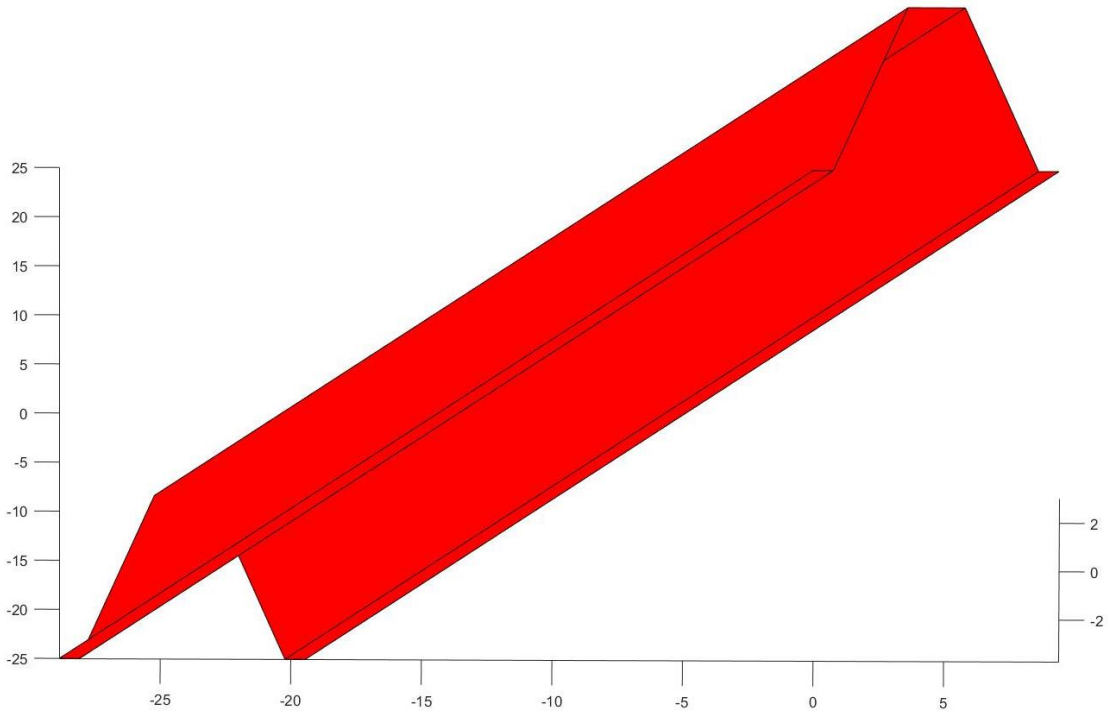

Figure 15.2: Rack vane in 3D

15.2 Results

The vane profile data is given as x, y coordinates in the $S_2(O_2, x_2, y_2, z_2)$ coordinate system represented in Figure (14.1).

Using equation (14.2) and matrix M_{12} for continuously incremented ϕ, it is possible to find the trajectory of the vane profile with respect to the $S_1(O_1, x_1, y_1, z_1)$ coordinate system.

By plotting those consecutive positions, the helical tooth shape on the work gear is generated as is shown in Figure (15.3).

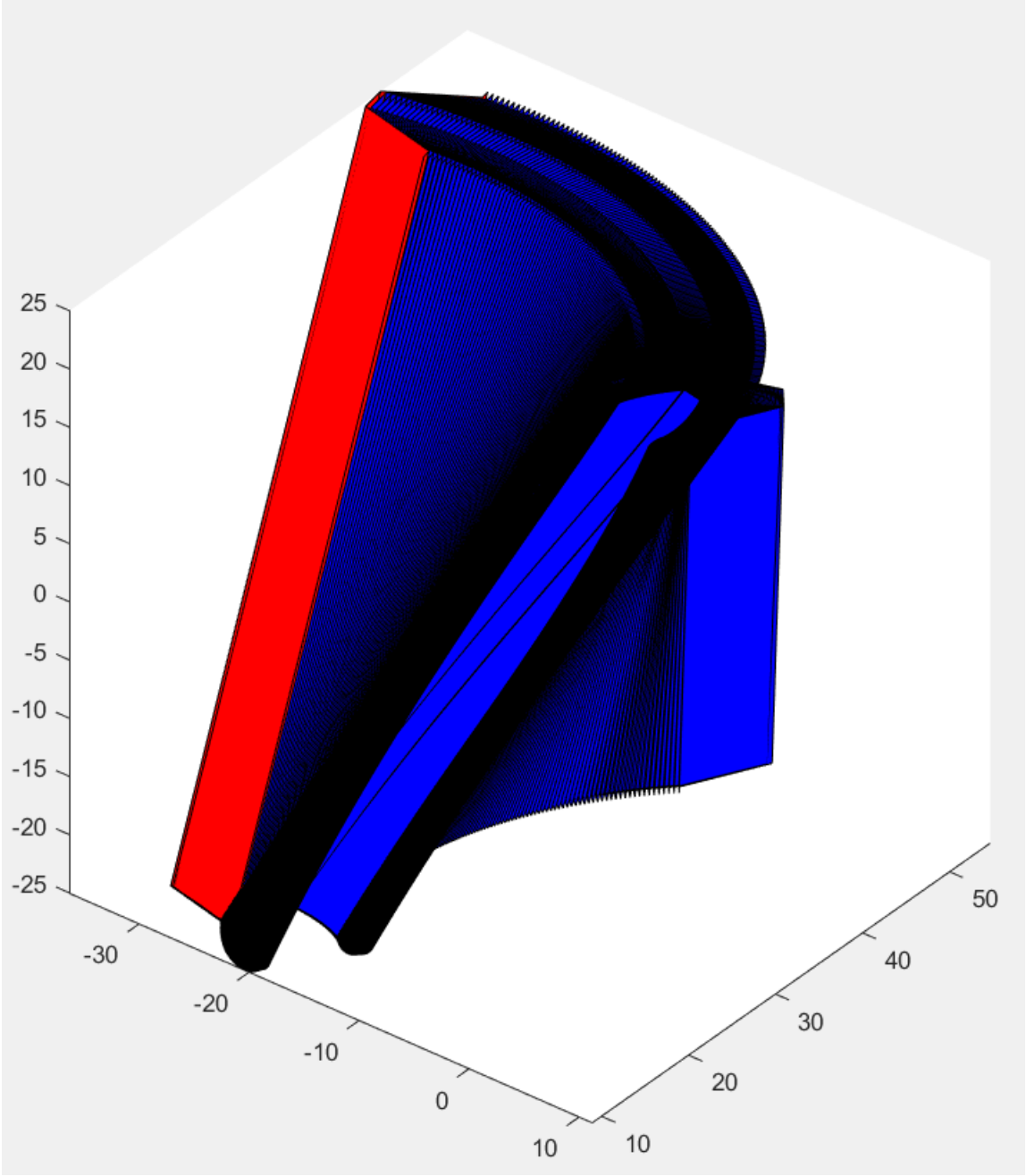

Figure 15.3: Generated tooth profile on the work gear

16. Alternative coordinate transformation for externally tangent helical gears

In the following is considered the unconventional cutting of a helical gear using a spur shaper cutter. This can be done due to helical gear teeth having a spur profile in their normal plane. A procedure similar to the one described in section (9) is used, adding to it a relative rotation of one of the two centrodes about the y axis with respect to the second centrode. The coordinate transformation would be as follows:

The relative rotation angles of the two centrodes does not depend exclusively on the radii in this scenario. Having figure (13.3) in mind, a normal angular pitch θ_{n1} of the spur cutter corresponds to a tangential angular pitch θ_{t2} of the blank helical gear. Combining equations (6.1) and (13.1),

$$\frac{\theta_{n1}}{\theta_{t2}} = \frac{p_n \rho_2}{p_t \rho_1} = cos\psi \frac{\rho_2}{\rho_1} \qquad \text{Equation 15.1}$$

The rotation angle ratio of the two centrodes is equal to their corresponding angular pitch ratio, therefore ϕ_1 and ϕ_2 are related by equation (15.2):

$$\frac{\phi_1}{\phi_2} = cos\psi \frac{\rho_2}{\rho_1} \qquad \text{Equation 15.2}$$

E is the shortest distance between the 2 axes of rotation. ($E = \rho_1 + \rho_2$)

To find the coordinates of points from centrode 2 to centrode 1, a coordinate transformation transition is required, and is based on the relation in the matrix equation (15.3):

$$r_1 = M_{12} r_2 = M_{1f} M_{fm} M_{mp} M_{p2} r_2 \qquad \text{Equation 15.3}$$

where M_{1f}, M_{mp} and M_{p2} are rotational matrices and M_{fp} is a translational matrix.

$$r_2 = \begin{bmatrix} x_2 \\ y_2 \\ z_2 \\ 1 \end{bmatrix}, \qquad r_1 = \begin{bmatrix} x_1 \\ y_1 \\ z_1 \\ 1 \end{bmatrix},$$

$$M_{1f} = \begin{bmatrix} cos\phi_1 & sin\phi_1 & 0 & 0 \\ -sin\phi_1 & cos\phi_1 & 0 & 0 \\ 0 & 0 & 1 & 0 \\ 0 & 0 & 0 & 1 \end{bmatrix}, \qquad M_{fm} = \begin{bmatrix} 1 & 0 & 0 & -E \\ 0 & 1 & 0 & 0 \\ 0 & 0 & 1 & 0 \\ 0 & 0 & 0 & 1 \end{bmatrix},$$

$$M_{mp} = \begin{bmatrix} 1 & 0 & 0 & 0 \\ 0 & cos\psi & -sin\psi & 0 \\ 0 & sin\psi & cos\psi & 0 \\ 0 & 0 & 0 & 1 \end{bmatrix}, \qquad M_{p2} = \begin{bmatrix} cos\phi_2 & sin\phi_2 & 0 & 0 \\ -sin\phi_2 & cos\phi_2 & 0 & 0 \\ 0 & 0 & 1 & 0 \\ 0 & 0 & 0 & 1 \end{bmatrix}.$$

It is assumed that positive angles are clockwise.

Equation (15.3) gives

$$M_{12} = \begin{bmatrix} cos\phi_1 cos\phi_2 + cos\psi sin\phi_1 sin\phi_2 & -cos\phi_1 sin\phi_2 + cos\psi sin\phi_1 cos\phi_2 & sin\psi sin\phi_1 & -E cos\phi_1 \\ -sin\phi_1 cos\phi_2 + cos\psi cos\phi_1 sin\phi_2 & sin\phi_1 sin\phi_2 + cos\psi cos\phi_1 cos\phi_2 & sin\psi cos\phi_1 & E sin\phi_1 \\ -sin\psi sin\phi_2 & -sin\psi cos\phi_2 & cos\psi & 0 \\ 0 & 0 & 0 & 1 \end{bmatrix}$$

The inverse transformation can be done using matrix $M_{21} = M_{12}^{-1}$ in equation (15.4):

$$r_2 = M_{21} r_1 \qquad \text{Equation 15.4}$$

Where

$$M_{21} = \begin{bmatrix} cos\phi_1 cos\phi_2 + cos\psi sin\phi_1 sin\phi_2 & -sin\phi_1 cos\phi_2 + cos\psi cos\phi_1 sin\phi_2 & -sin\psi sin\phi_2 & Ecos\phi_1 \\ cos\phi_1 sin\phi_2 + cos\psi sin\phi_1 cos\phi_2 & sin\phi_1 sin\phi_2 + cos\psi cos\phi_1 cos\phi_2 & -sin\psi cos\phi_2 & -Esin\phi_1 \\ sin\psi sin\phi_1 & sin\psi cos\phi_1 & cos\psi & 0 \\ 0 & 0 & 0 & 1 \end{bmatrix}$$

17. Alternative application for parallel helical gears

17.1 Data given

The spur shaper cutter used in this application has the same tooth profile as the one used in Section (12) and is shown in Figures (17.1) and (17.2).

➢ The shaper cutter data is as follows:

- Tooth profile is shown in Figure (12.1)
- Number of teeth: $N_1 = 17$
- Module: $m = 3$
- Pressure angle: $\alpha = 20^o$
- Addendum: $a_1 = 1.3m$
- Dedendum: $b_1 = 1m$
- Radius: $R_1 = \frac{mN_1}{2} = 25.5$

➢ Target dimensions for the blank gear:

- Radius: $R_2 = R_1 = 25.5$
- Number of teeth: $N_2 = N_1 = 17$
- Normal pressure angle: $\alpha_n = 20^o$
- Normal module: $m_n = 3$
- Helix angle: $\psi = 10^o$

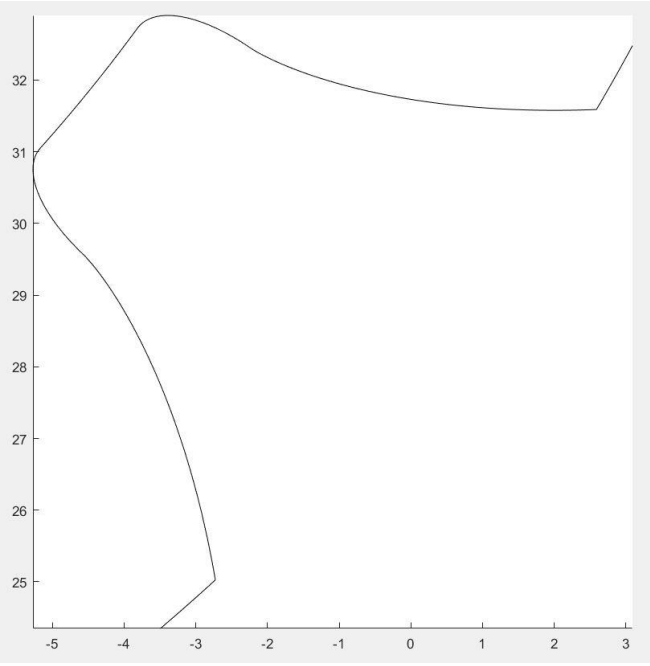

Figure 17.1: Shaper cutter vane profile

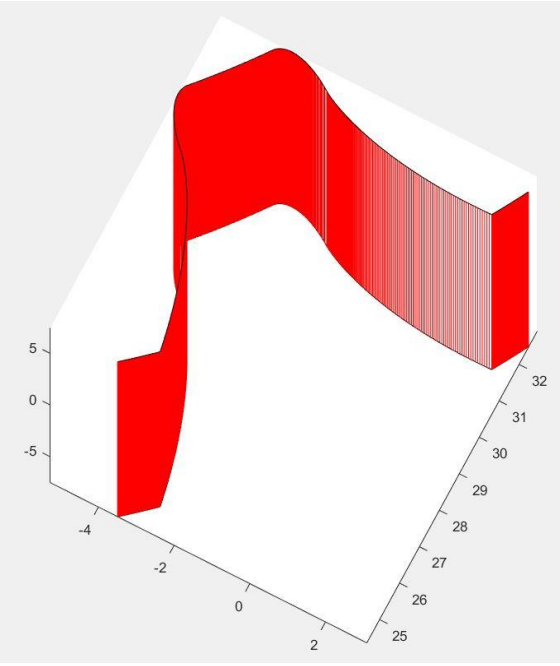

Figure 17.2: Shaper cutter vane (3D)

17.2 Results

The vane profile data is given as x, y, z coordinates in the $S_2(O_2, x_2, y_2, z_2)$ coordinate system. Using equation (16.3) and matrix M_{12} for continuously incremented ϕ angles (always in relation according to equation (16.2)), it is possible to find the trajectory of the vane profile with respect to the $S_1(O_1, x_1, y_1, z_1)$ coordinate system.

By plotting those consecutive positions, the tooth profile on the work gear is generated as is shown is Figure (17.3).

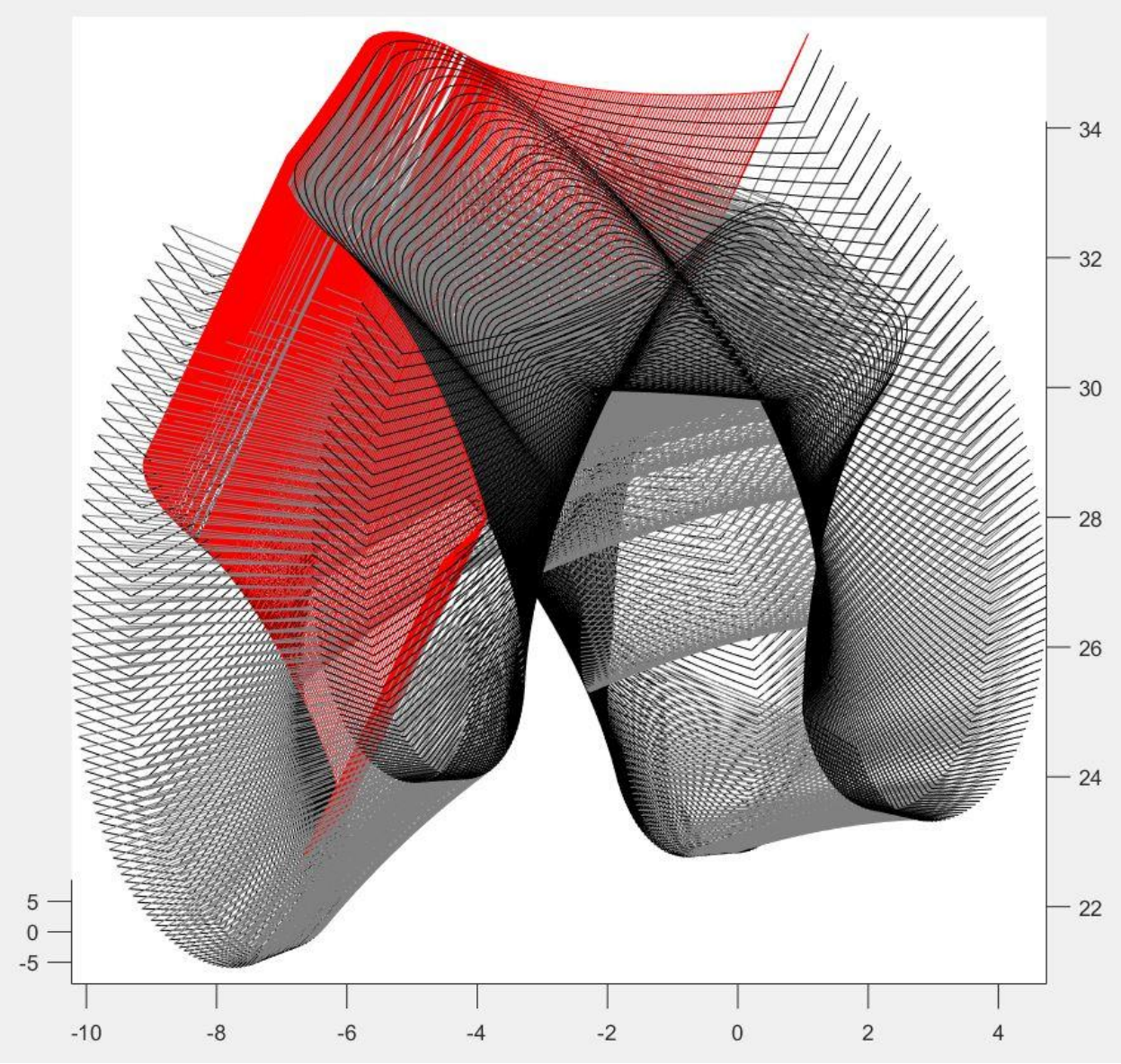

Figure 17.3: Generated helical tooth

With reference to Figure (13.3), it is possible to generate to envelope tooth profiles in both the corresponding sections *A-A* and *B-B* of the generated helical gear.

Section *B-B* is characterized by a tooth profile identical to the one generated by the cutting process of a spur gear with the same shaper cutter, and is shown in Figure (17.5).

Section *A-A* is characterized by a tooth profile similar to the one in cross section *B-B* but slightly stretched in the tangential direction, and is shown in Figure (17.4).

Effectively, section *B-B* is the projection of section *A-A* along an angle equal to the *helix angle* ψ.

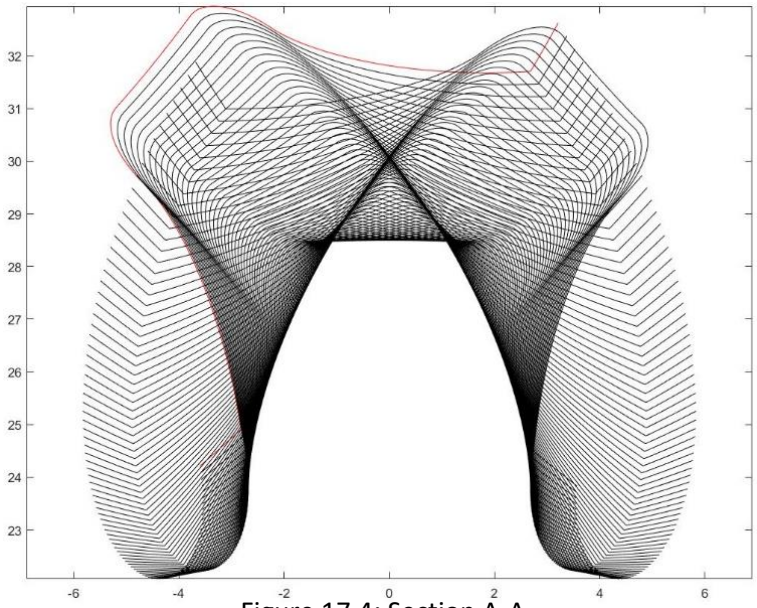

Figure 17.4: Section A-A

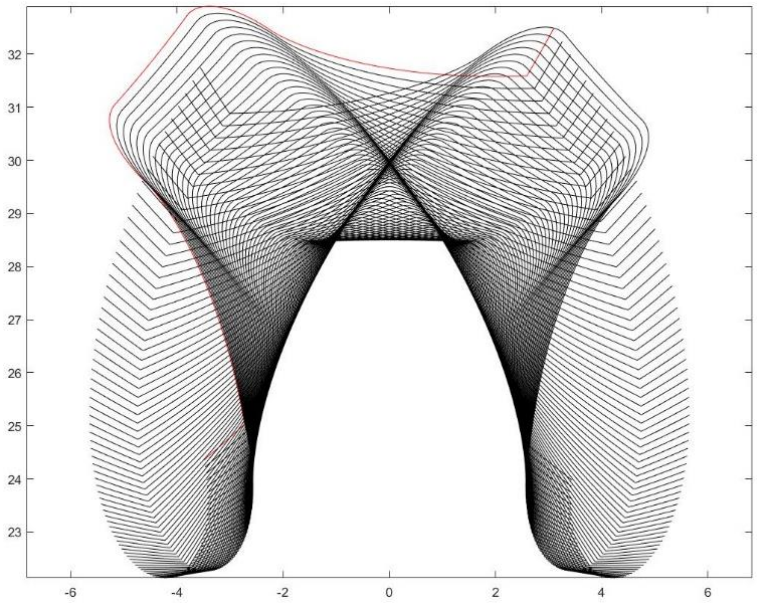

Figure 17.5: Section B-B

18. Face Gears

A Face-Gear Drive is used to transmit a rotational motion between crossed or intersected axes. Conventionally, a face-gear drive combines a spur pinion with its conjugate face-gear.

Figure 18.1: Face-gear drive

When generating a face-gear with a shaper, contact between the shaper surface and the face gear surface is always a *contact line*. If the pinion using in the application is identical to the shaper that generated the face-gear, the whole assembly will be extremely sensitive to misalignment, which can translate in an undesirable shift of the bearing contact and even a separation of the surfaces. This is why it is important to provide a *point contact* rather than a *line contact* between the pinion and the face-gear, which leads to a localized bearing contact and an assembly less sensitive to misalignment.

Point contact between the pinion and the face-gear can be provided by using a shaper with a greater number of teeth N_s than that of the pinion N_p to be used in the application.

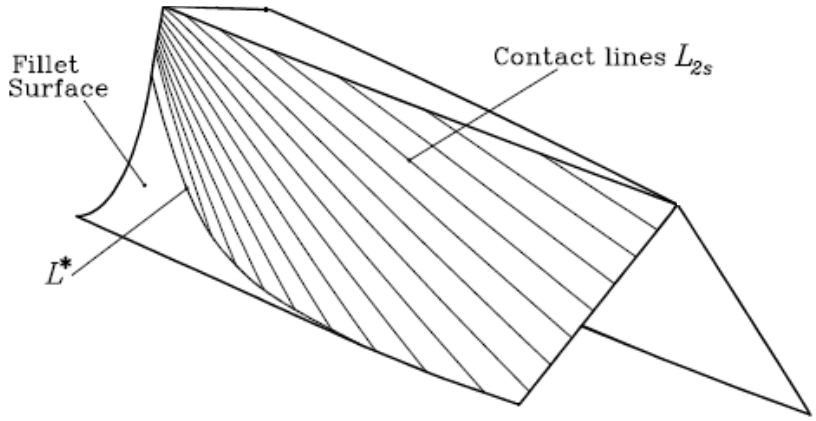

Figure 18.2: Structure of face-gear tooth

The structure of a face-gear tooth is shown in Figure (18.2). The tooth is divided in two parts: the working part made by the contact lines L_{2s} that are the tangency lines between the shaper and the face-gear, and the fillet surface generated by the top edge of the shaper. L^* is the common line between the working line and the fillet surface.

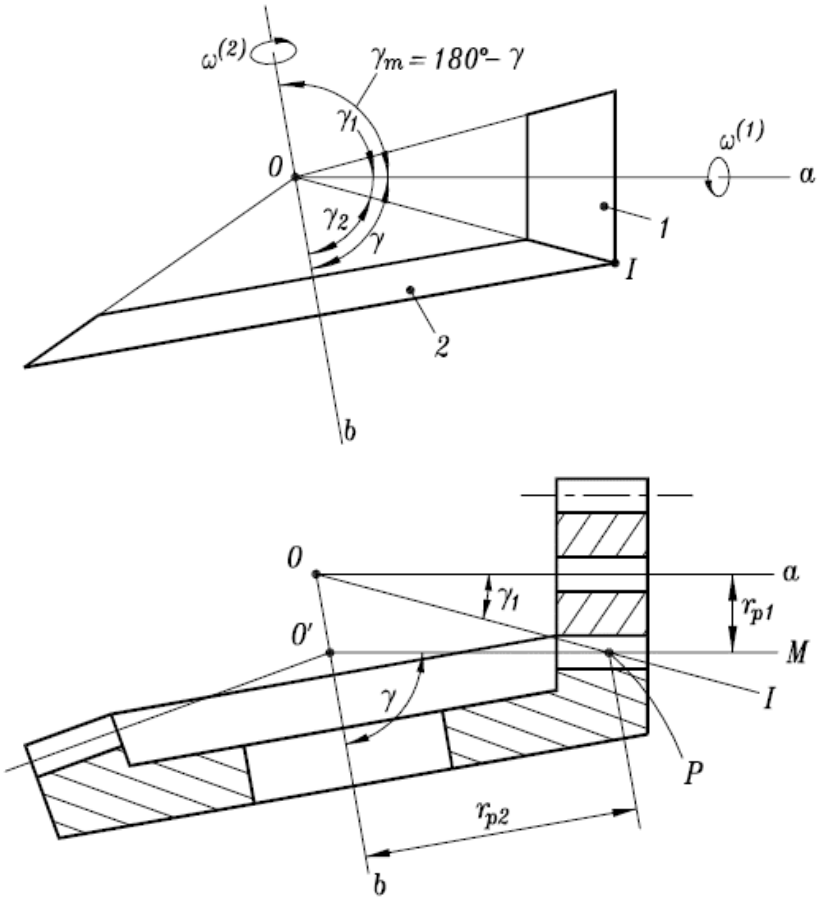

Figure 18.3: Axodes and pitch cones

Figure (18.3) shows schematics of a face-gear drive. The pinion and the face-gear rotate about axes *Oa* and *Ob* respectively. The gear ratio is defined in equation (18.1)

$$m_{12} = \frac{\omega_1}{\omega_2} = \frac{N_2}{N_1} \qquad \text{Equation 18.1}$$

where ω_i and N_i are respectively the rotational speed and the number of teeth of the pinion ($i = 1$) and the face-gear ($i = 2$). The *axodes* are the two cones of semi-angles γ_1 and γ_2 defined in equations (18.2) and (18.3)

$$cot\gamma_1 = \frac{m_{12} + cos\gamma}{sin\gamma} \qquad \text{Equation 18.2}$$

$$cot\gamma_2 = \frac{m_{21} + cos\gamma}{sin\gamma} = \frac{1 + m_{12} cos\gamma}{m_{12} sin\gamma} \qquad \text{Equation 18.3}$$

where $m_{21} = \frac{1}{m_{12}}$.

The line OI is the line of tangency of the axodes and the *instantaneous axis of rotation* in relative motion of the pinion and face-gear. An axode is the family of instantaneous axes of rotation that is generated in coordinate systems rigidly attached to the pinion and gear. The axodes are the *pitch cones* of the bevel gear drive and are the basis for designing a bevel gear drive.

The *pitch surfaces* of a face-gear drive are the cylinder of radius r_{p1} (pitch surface of the pinion) and the cone of semi-angle γ (the pitch surface of the face-gear) shown in Figure (18.3). For $\gamma = 90^{o}$, the face-gear corresponds to a flat plane.

The *pitch line* is $O'M$. It is the tangency line between the pitch surfaces.

The *pitch point* P is the intersection of the pitch line $O'M$ with the instantaneous axis of rotation OI. The relative motion of the pinion and the face-gear at point P is pure rolling, whereas it is sliding and rolling at other points of the pitch line $O'M$.

The generation process of a face-gear is similar to any other gear forming by shaping. It is an exact meshing simulation where the shaper cutter is an identical copy of the pinion. Both the cutter and the blank gear are rotated with relative angular velocities following Equation (18.4), and the cutter also performs a reciprocating motion in the direction of the generatrix of the face-gear cone which is parallel to the axis of the shaper cutter.

$$\frac{\omega_s}{\omega_2} = \frac{N_2}{N_s} \qquad \text{Equation 18.3}$$

where index $i = s$ refers to the shaper, and index $i = 2$ refers to the blank face-gear.

It is worth re-iterating generating a cutter identical to the pinion generates a face-gear drive that is sensitive to misalignment, which is why the bearing contact between the face-gear and the pinion must be localized, and the *line of contact* must be replaced by an instantaneous *point contact*.

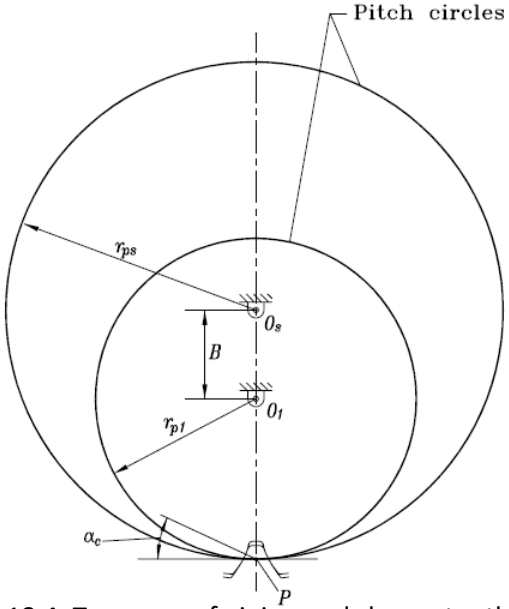

Figure 18.4: Tangency of pinion and shaper tooth profiles

The reasoning behind the localization of the bearing contact is summarized in as follows:

- The shaper cutter number of teeth N_s must be larger than the number of teeth of the pinion N_1. Generally, $N_s - N_1 = 2 \; or \; 3$.
- The pinion and shaper are simulated to have an imaginary internal meshing as shown in Figure (18.4).

- In the previously mentioned meshing, the axodes of the shaper and pinion are the pitch cylinders of radii r_{ps} and r_{p1} (Figure 18.4). The common tangent to the pitch cylinders is parallel to their axes of rotation and passes through the pitch point P. This common tangent is in fact the instantaneous axis of rotation IA_{s1} (Figure 18.5) in the relative motion of the pinion with respect to the shaper.

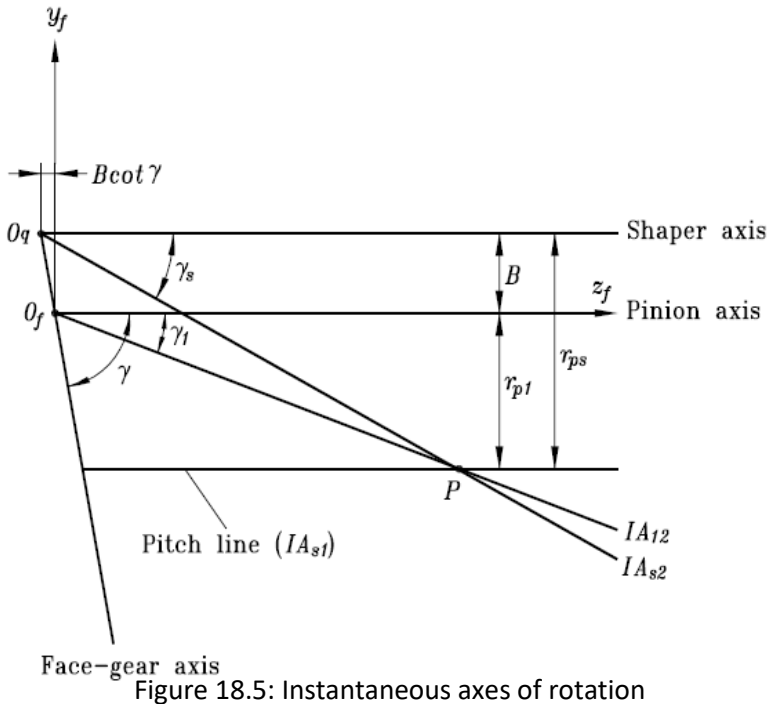

Figure 18.5: Instantaneous axes of rotation

- Three surfaces can be considered in mesh simultaneously:
  - Surface Σ_1 corresponding to the generated face-gear.
  - Surface Σ_2 corresponding to the pinion.
  - Surface Σ_s corresponding to the shaper.

Surfaces Σ_s and Σ_2 are in *line contact* throughout the shaping of the face-gear. Surfaces Σ_s and Σ_1 are in *line contact* throughout the imaginary meshing of the shaper and the pinion. Surfaces Σ_1 and Σ_2 are in *point contact* throughout the meshing.

- Figure (18.5) shows the instantaneous axes of rotation in the meshing of the three surfaces Σ_1, Σ_2 and Σ_s. They are designated by IA_{s1}, IA_{s2} and IA_{12} indicating the respective meshings between Σ_s and Σ_1, Σ_s and Σ_2, and Σ_1 and Σ_2. The angle γ_s formed between the shaper axis and IA_{s2} is determined by Equation (18.4)

$$cot\gamma_s = \frac{m_{s2}+cos\gamma}{sin\gamma} = \frac{\frac{N_2}{N_s}+cos\gamma}{sin\gamma} \qquad \text{Equation 18.4}$$

which is similar to Equation (18.2) to determine γ_1. IA_{s1} coincides with the *pitch line*. All three instantaneous axes of rotation intersect at the *pitch point* P. B is the shortest distance between the axes of rotation of the pinion and the shaper and can be determined according to Equation (18.5)

$$B = r_{ps} - r_{p1} = \frac{N_s - N_1}{2P_d} \qquad \text{Equation 18.5}$$

19. Coordinate transformation for face-gears

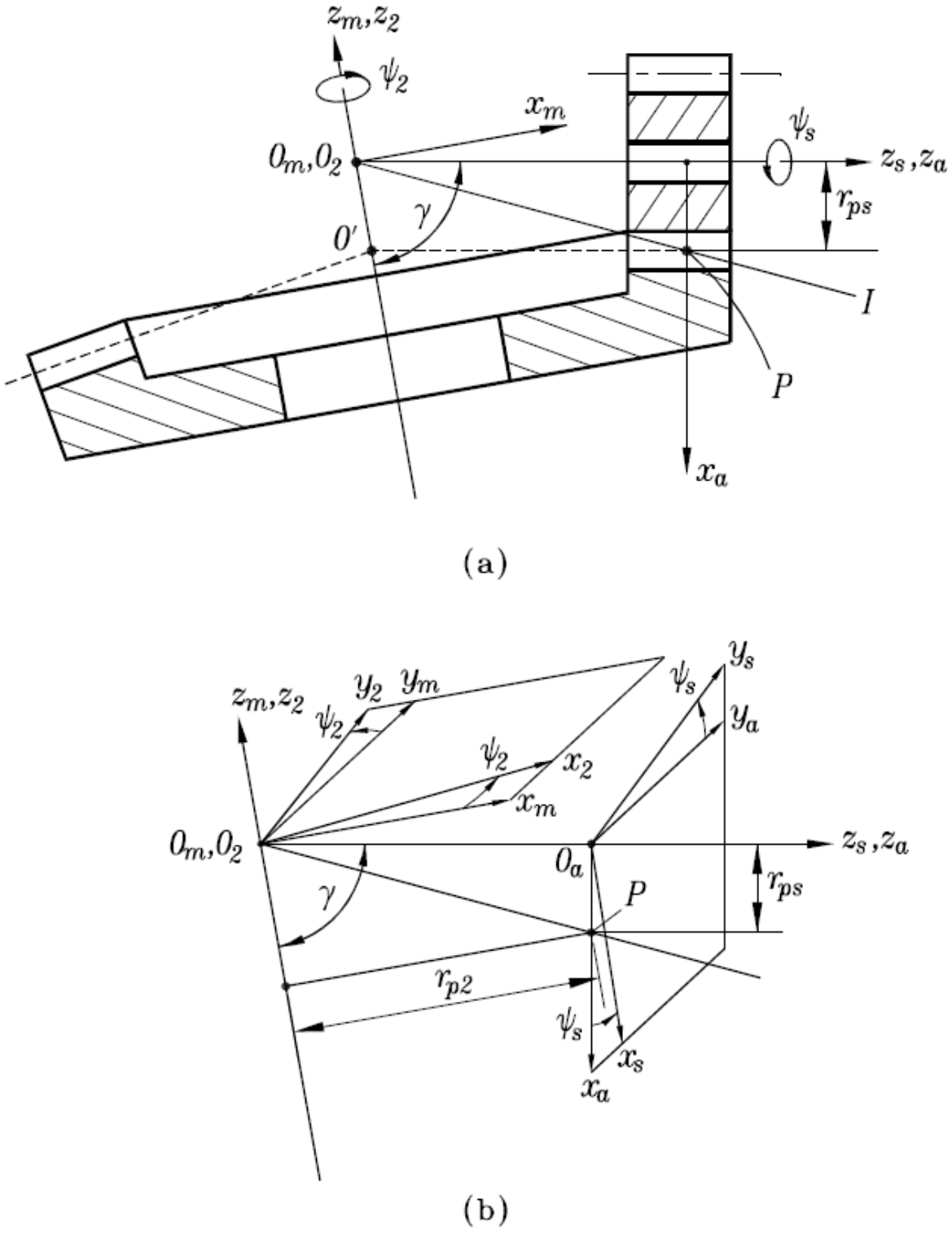

Figure 19.1: Coordinate system for generation of face-gear surface: (a) illustration of installation; (b) derivation of coordinate transformation

The surface Σ_2 of the generated face-gear is the envelope of the family of shaper tooth surfaces Σ_s are rotate about their axis of rotation.

In Figure (19.1) are shown 4 coordinate systems:

- $S_s(O_a, x_s, y_s, z_s)$ is the primary coordinate system rigidly connected to rotating shaper gear.
- $S_2(O_2, x_2, y_2, z_2)$ is the primary coordinate system rigidly connected to rotating blank face-gear.
- $S_m(O_m, x_m, y_m, z_m)$ is an auxiliary coordinate system rigidly connected to the gear housing.
- $S_a(O_a, x_a, y_a, z_a)$ is an auxiliary coordinate system rigidly connected to the gear housing.

Coordinate axis $O_a x_a$ passes through the *pitch point P*.

During the shaping process, the shaper rotates about axis z_a and the blank face-gear about axis z_m according to the relation in Equation (19.1)

$$\frac{\psi_s}{\psi_2} = \frac{N_2}{N_s} \qquad \text{Equation 19.1}$$

The family of shaper surfaces is based off the matrix Equation (19.2)

$$r_2 = M_{2s} r_s = M_{2m} M_{ma} M_{as} r_s \qquad \text{Equation 19.2}$$

where:

$$M_{as} = \begin{bmatrix} cos\psi_s & -sin\psi_s & 0 & 0 \\ sin\psi_s & cos\psi_s & 0 & 0 \\ 0 & 0 & 1 & 0 \\ 0 & 0 & 0 & 1 \end{bmatrix}, \qquad M_{ma} = \begin{bmatrix} -cos\gamma & 0 & sin\gamma & r_{p2} \\ 0 & 1 & 0 & 0 \\ -sin\gamma & 0 & -cos\gamma & -r_{p2}cot\gamma \\ 0 & 0 & 0 & 1 \end{bmatrix},$$

$$M_{2m} = \begin{bmatrix} cos\psi_2 & sin\psi_2 & 0 & 0 \\ -sin\psi_2 & cos\psi_2 & 0 & 0 \\ 0 & 0 & 1 & 0 \\ 0 & 0 & 0 & 1 \end{bmatrix}, \qquad r_s = \begin{bmatrix} x_s \\ y_s \\ z_s \\ 1 \end{bmatrix}, \qquad r_2 = \begin{bmatrix} x_2 \\ y_2 \\ z_2 \\ 1 \end{bmatrix}.$$

Equation (19.2) gives

$$M_{2s} = \begin{bmatrix} -cos\psi_2 cos\gamma cos\psi_s + sin\psi_2 sin\psi_s & cos\psi_2 cos\gamma sin\psi_s + sin\psi_2 cos\psi_s & cos\psi_2 sin\gamma & r_{p2} cos\psi_2 \\ sin\psi_2 cos\gamma cos\psi_s + cos\psi_2 sin\psi_s & -sin\psi_2 cos\gamma sin\psi_s + cos\psi_2 cos\psi_s & -sin\psi_2 sin\gamma & -r_{p2} sin\psi_2 \\ -sin\gamma cos\psi_s & sin\gamma cos\psi_s & -cos\gamma & -r_{p2} cot\gamma \\ 0 & 0 & 0 & 1 \end{bmatrix}$$

20. Application for face-gears

20.1 Data given

The same spur shaper cutter defined in Section (12) is still being used in this application with its vane profile shown in Figure (20.1)

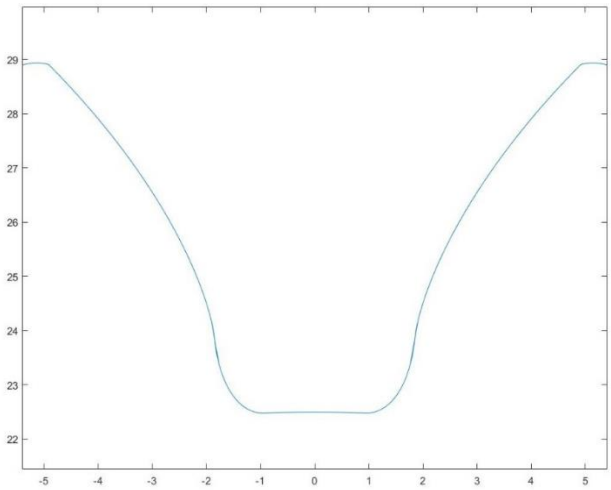

Figure 20.1: Shaper cutter gear vane profile

➢ The shaper cutter data is as follows:

- Number of teeth: $N_1 = 17$
- Module: $m = 3$
- Pressure angle: $\alpha = 20^o$
- Radius: $R_1 = \frac{mN_1}{2} = 25.5$

➢ Target dimensions for the blank face-gear:

- Radius: $R_2 = 10R_1 = 255$
- Number of teeth: $N_2 = 10N_1 = 170$

20.2 Results

The spur gear shaper cutter vane profile data is given as x, y coordinates in the $S_s(O_a, x_s, y_s, z_s)$ coordinate system represented in Figure (19.1).

Using equation (19.2) and matrix M_{12} for continuously incremented ψ_s and ψ_2 always according to equation (19.1), it is possible to find the trajectory of the vane profile with respect to the $S_2(O_2, x_2, y_2, z_2)$ coordinate system.

By plotting those consecutive positions, the tooth profile on the blank face-gear is generated as is shown in Figure (20.2).

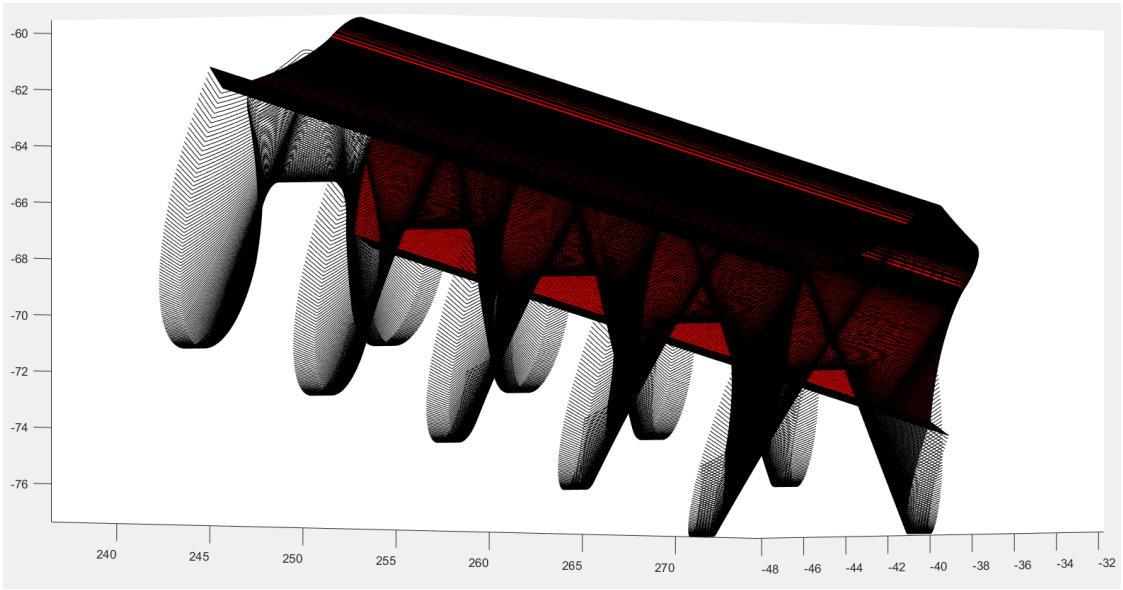

Figure 20.2: Generated face-gear tooth profiles

Figure (20.2) shows five equidistant profiles of the generated face-gear tooth, highlighting the continuously changing tooth profile in such an application. The tooth profile on the left of Figure (20.2) is close to the spur vane profile (the inside of the face-gear) and gradually takes a triangular shape moving to the right side of the figure (the outside of the face-gear).

21. Envelope of Internal Spur Gears

This section builds upon an already existing Matlab code used to generate the envelope of an external spur gear via a shaping procedure.

The code takes in as input all the various parameters of the desired spur gear, then it generates the geometry of the rack required to form the desired spur gear geometry. The code then takes in the relative motion of the rack cutter and the blank gear in a way analogous to what was previously detailed in Section 14.

Figure (21.1) shows the rack geometry, Figure (21.2) shows the relative motion of the pair or gears, and Figure (21.3) shows the corrected envelope of the spur gear generated by this shaping process. This same envelope is also represented by the blue line in Figure (21.2).

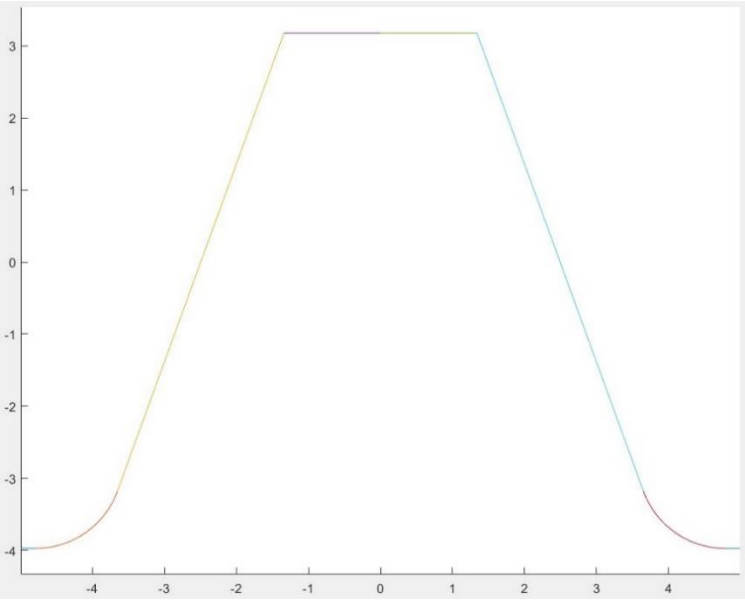

Figure 21.1: Rack geometry (vane)

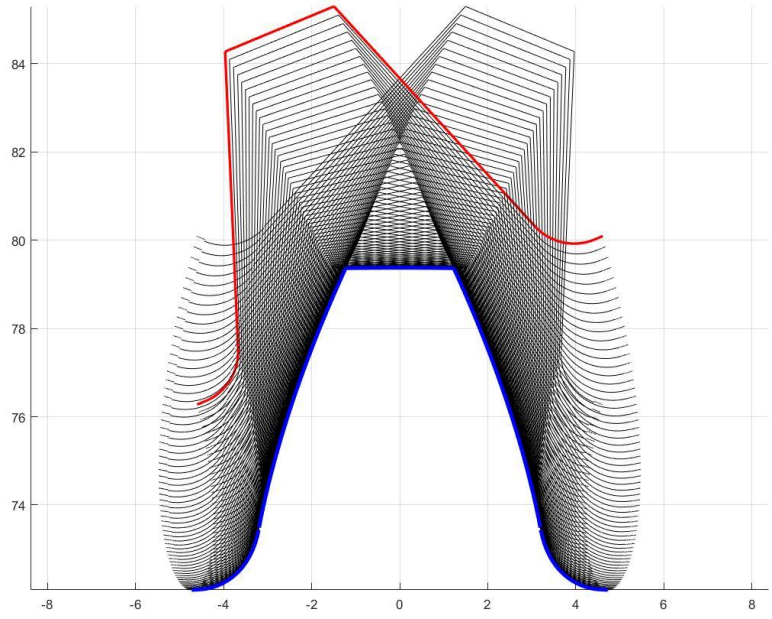

Figure 21.2: Relative motion

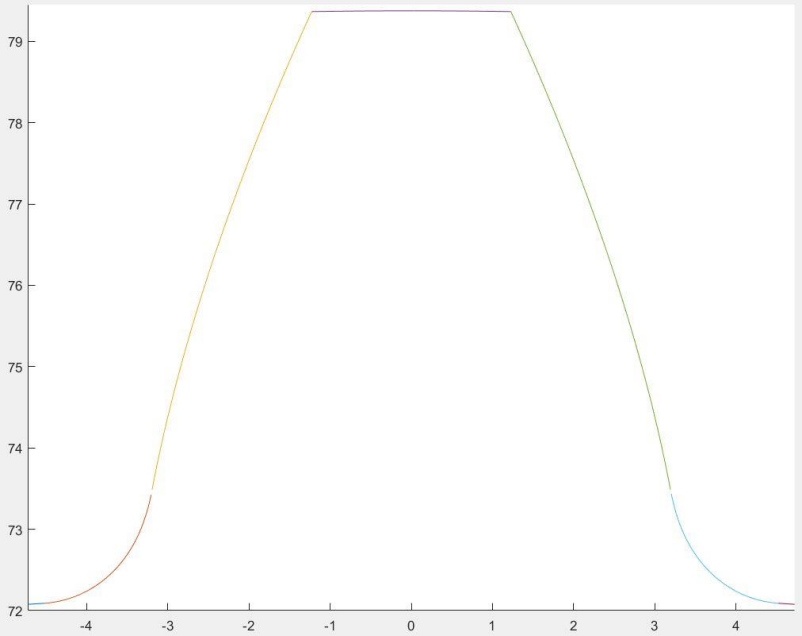

Figure 21.3: Envelope of the generated spur gear tooth

Generating the envelope is based on the theorem that states that a point of the cutter generates a respective point on the blank gear if the normal to the profile of the cutter at that point passes through the instantaneous center of rotation, also known as the *Pitch Point P* (shown in Figure 5.1). Figure (21.4) shows some normals (green arrows) of the cutter profile used in Figure (21.2).

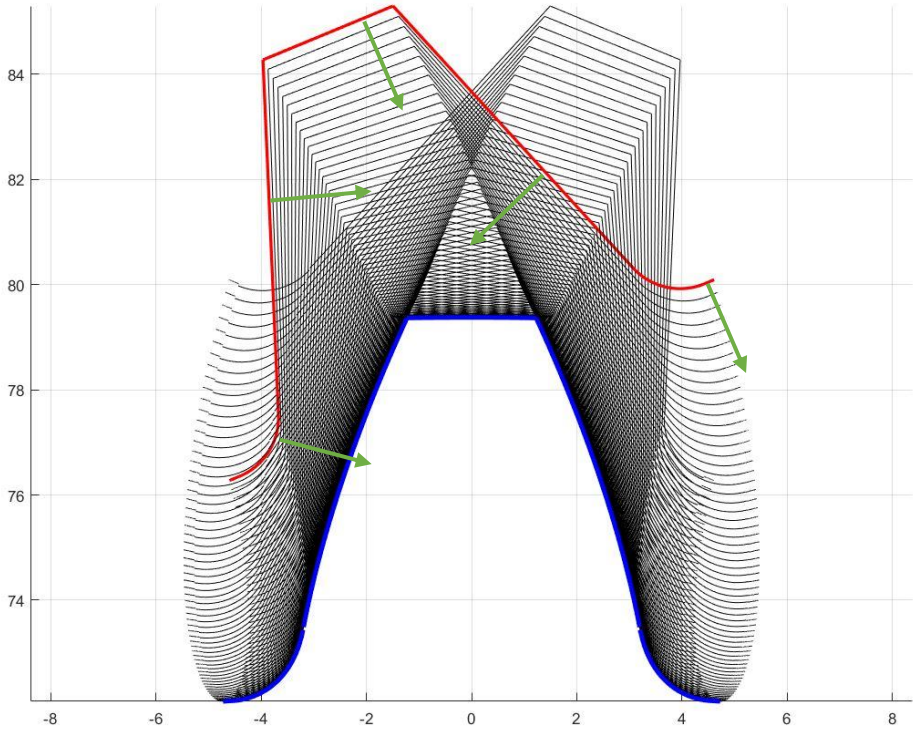

Figure 21.4: Normals of the cutter profile

The additions and modifications done to the code consist in using the output (spur gear profile) as the pinion shaper cutter of an internal spur gear. The spur tooth profile (Figure 21.3) has to be first transformed into a vane as is shown in Figure (21.5)

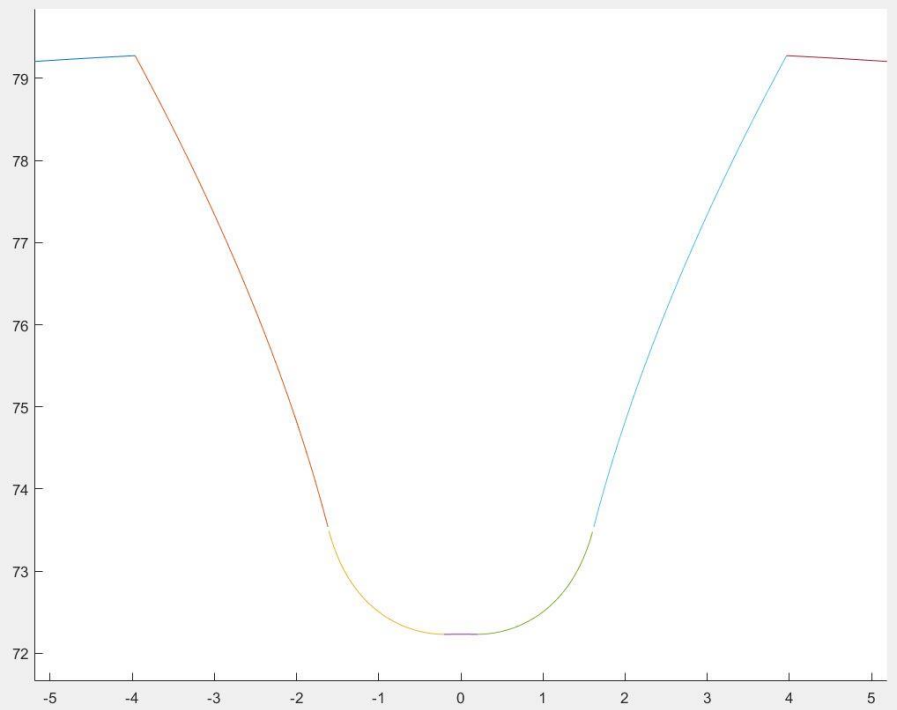

Figure 21.5: Vane profile

Relative motion is then administered to the vane profile. Results are shown in Figure (21.6)

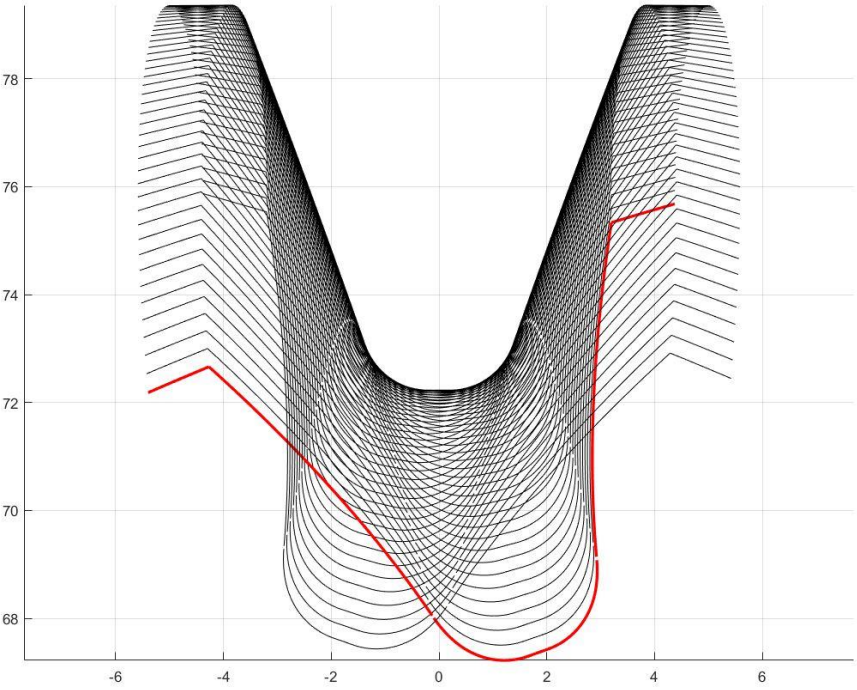

Figure 21.6: Relative motion for the internal gear shaping

By applying the aforementioned theorem to generate the envelope curve, we obtain a plot that is missing the two fillets at the root of the tooth, shown in Figure (21.7)

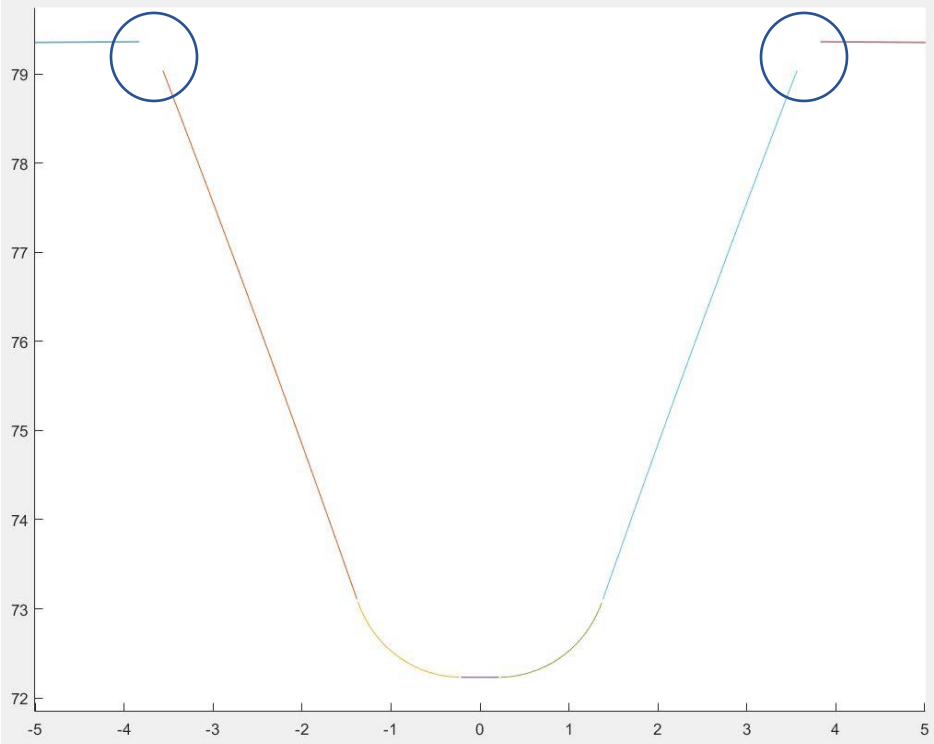

Figure 21.7: Internal gear tooth profile

The solution to this problem lies at the angular tip of the shaper cutter. The missing fillet is the portion of the internal gear tooth profile that is generated by the angular tip of the cutter. The normals to the cutter profile show a sudden change in direction at the angular tip, which results in an inaccurate normal at the angular point.

A proposed solution to this issue is to have a variable normal direction at the tip, ranging within an interval of values delimited by the normal directions of the two adjacent points to the angular tip as is shown in Figure (21.8). The generated points that fit the previously mentioned theorem would be grouped with the other points of the envelope, pending a correction. Figure (21.9) shows the uncorrected envelope resulting from the presented solution.

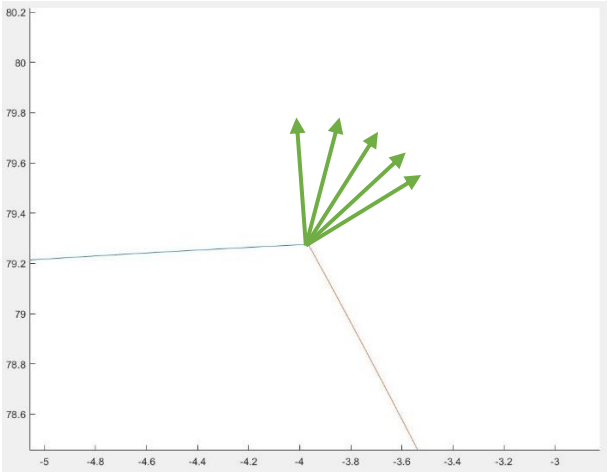

Figure 21.8: Normals at the angular tip

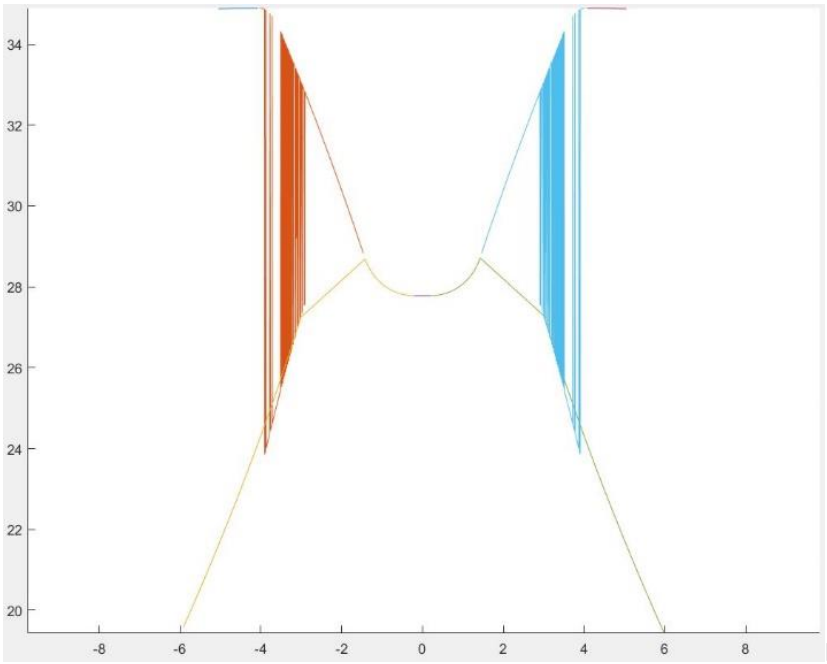

Figure 21.9: Uncorrected envelope

It is obvious that many generated points do not belong to the envelope, and it is evident that among them, any point whose radius is smaller than the radius of the center point of the envelope does not belong to the envelope. Once those points are removed, the results look like Figure (21.10).

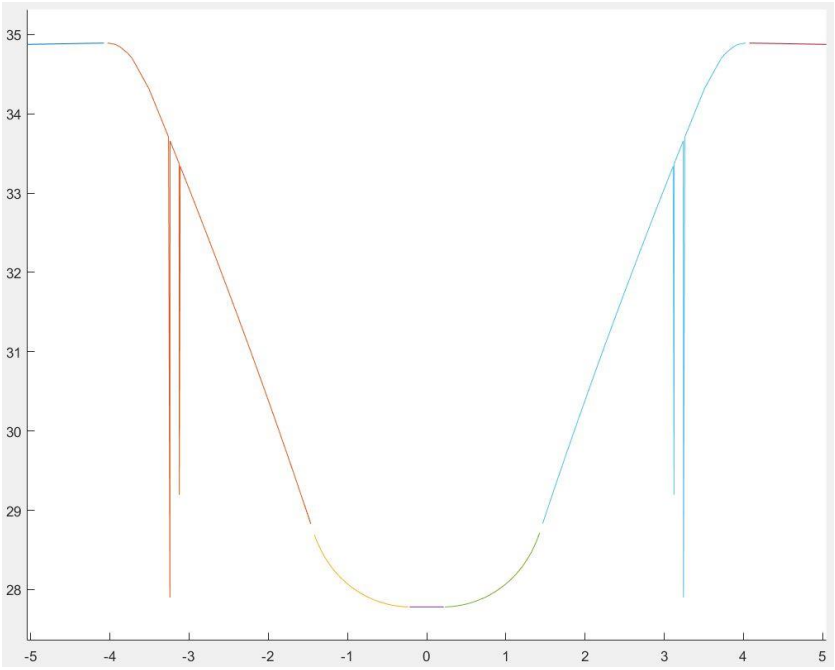

Figure 21.10: First correction of the envelope

Few points remain to be removed from the generated envelope, which is easily doable by deleting points that are fairly distant from the previous point on the envelope. The fully-corrected envelope is presented in Figure (21.11). Figure (21.12) shows the relative cutter-blank motion combined with the finished envelope.

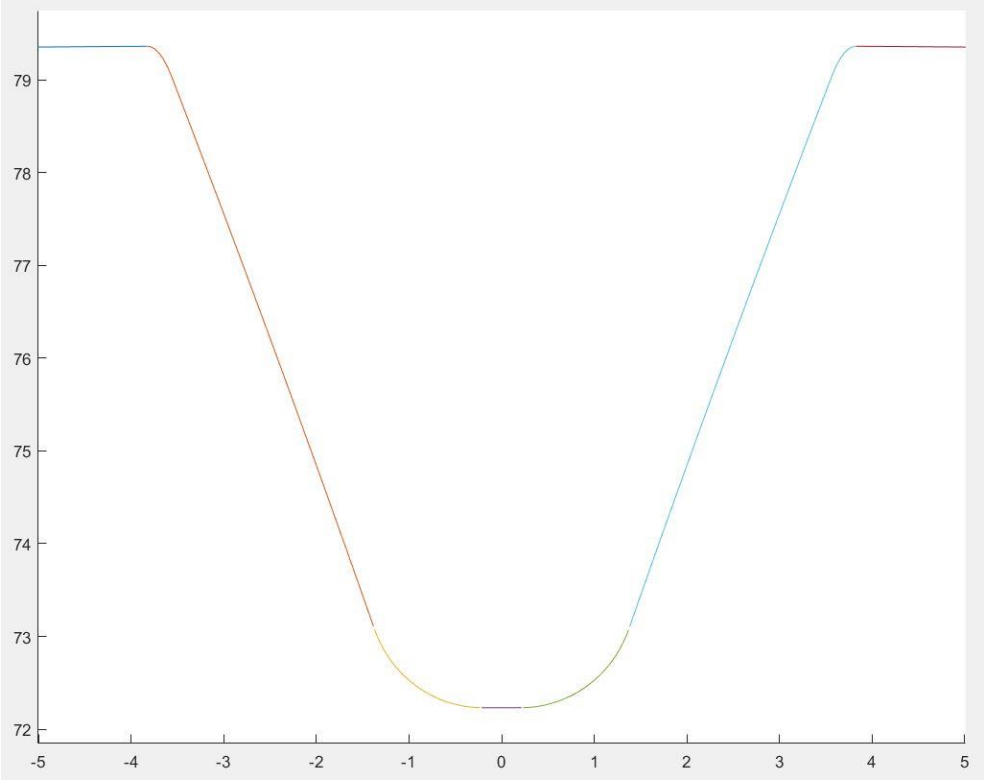

Figure 21.11: Second correction of the envelope

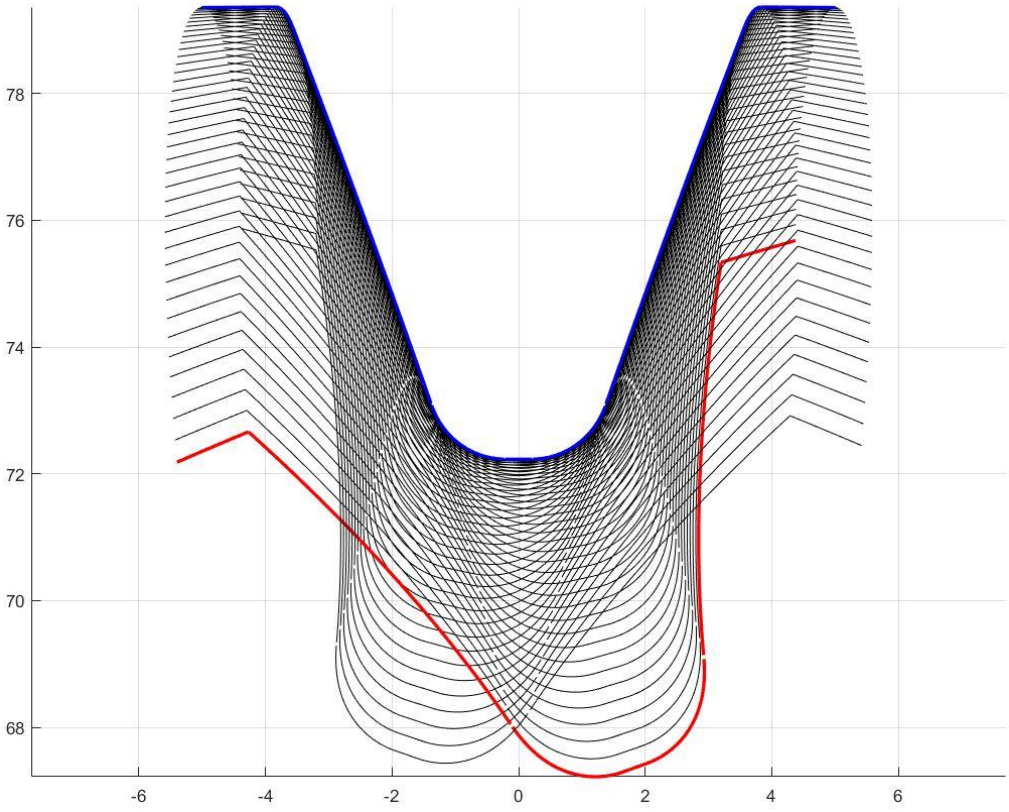

Figure 21.12: Final Result, relative motion and generated envelope

Figure (21.12) has a shaper cutter with the following data:

- Number of teeth: 48
- Gear ratio: 8
- Pressure angle: 20^{o}
- Module: 3.125
- Root fillet coefficient: 0.38
- Addendum: 1m
- Dedendum: 1.25m

Here are presented some other results with one different parameter in each case. The other parameters are identical to the previous case.

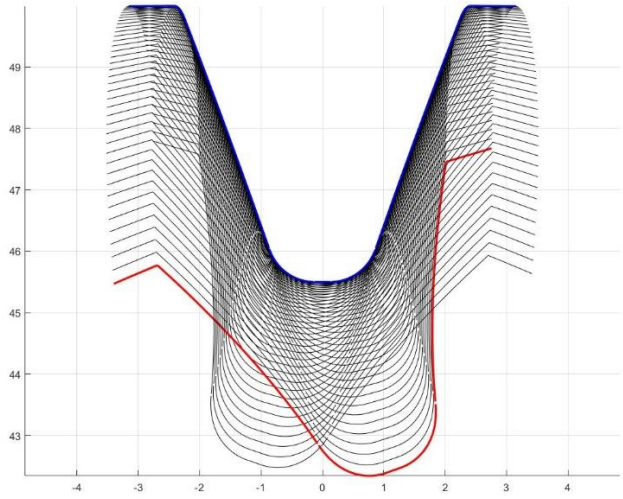

Figure 21.13: Module = 2

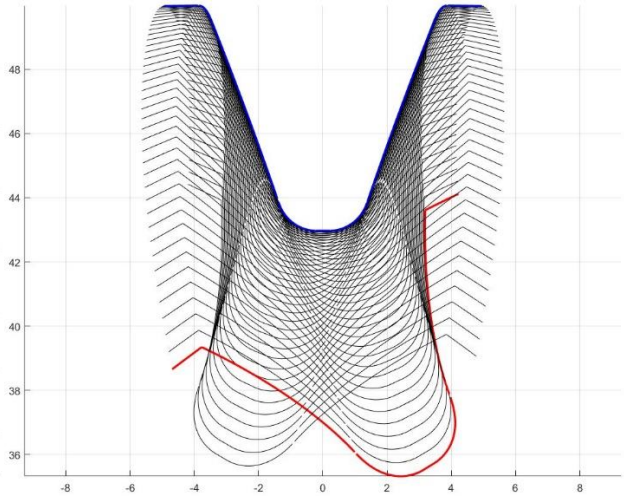

Figure 21.14: Number of teeth = 30

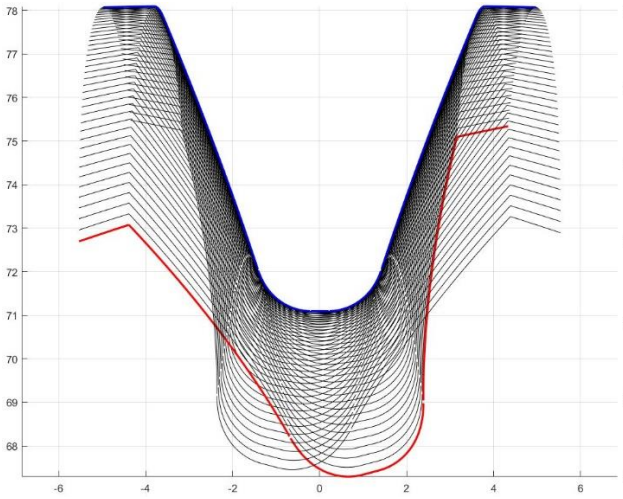

Figure 21.15: Gear ratio = 3

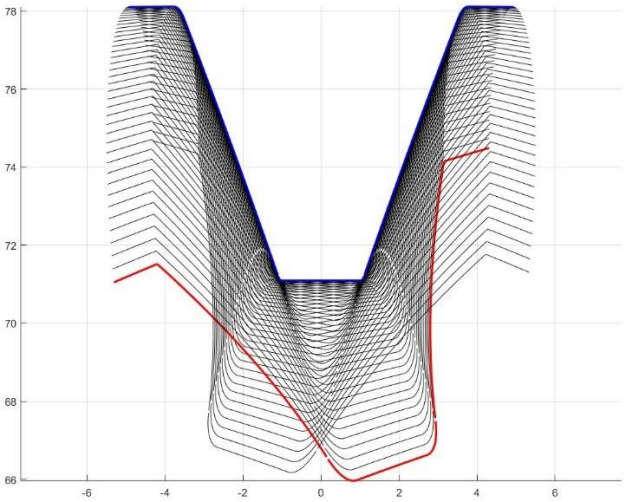

Figure 21.16: Root fillet coefficient = 0.01

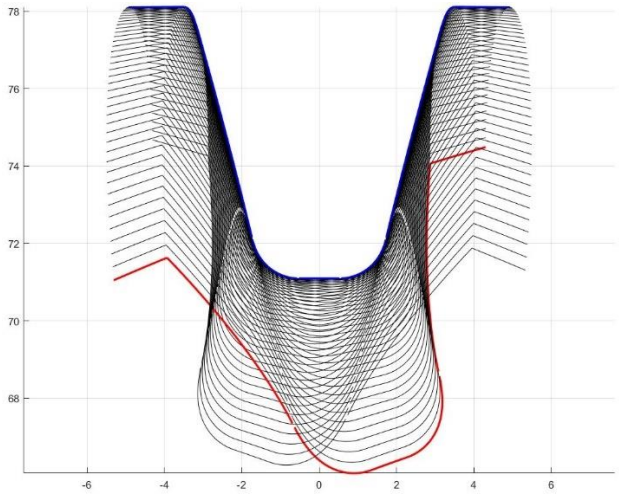

Figure 21.17: Pressure angle = 14.5°

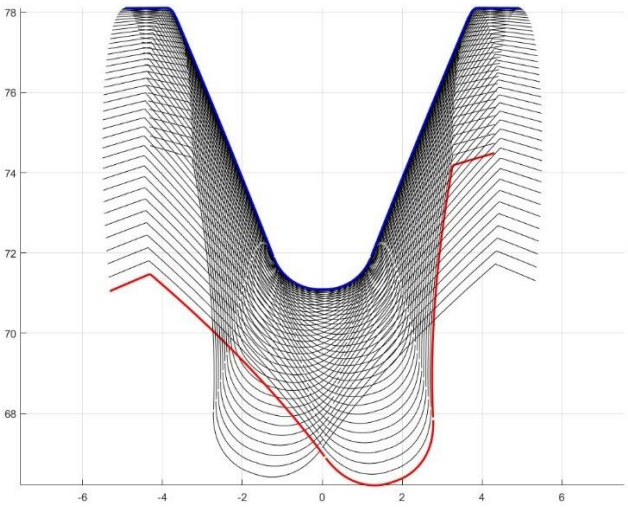

Figure 21.18: Pressure angle = 22°

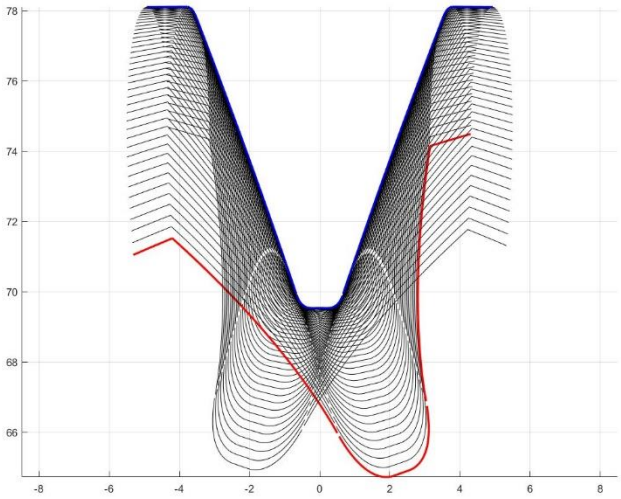

Figure 21.19: Addendum = 1.75m

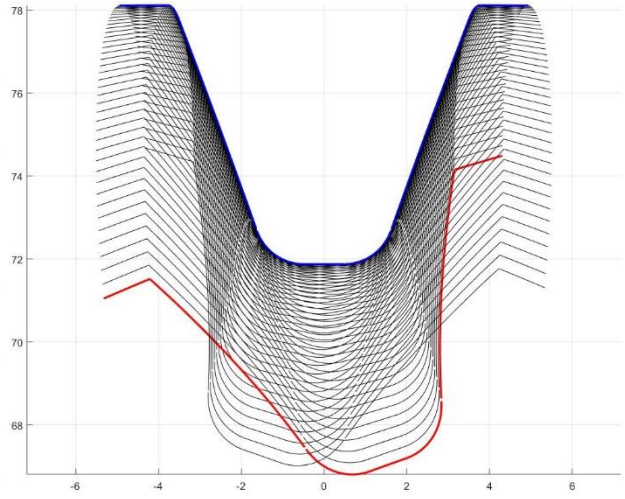

Figure 21.20: Addendum = 1m

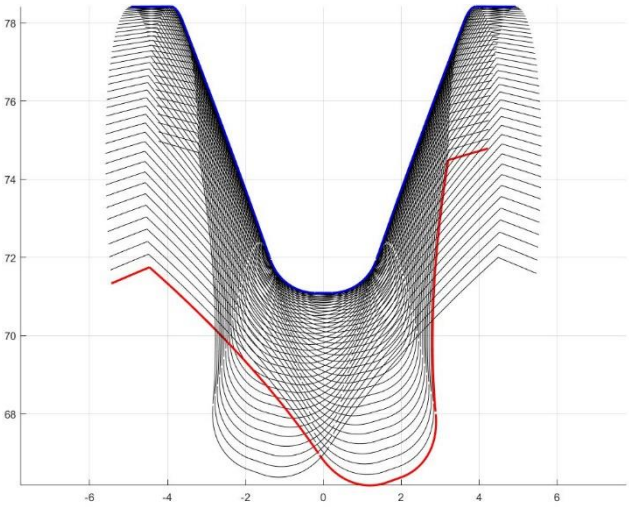

Figure 21.21: Dedendum = 1.1m

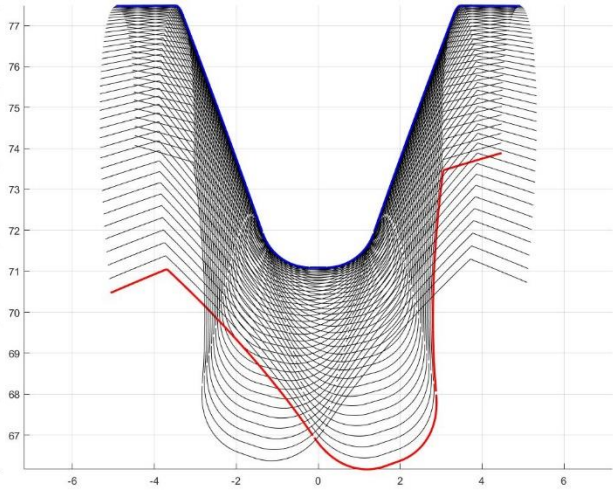

Figure 21.22: Dedendum = 0.8m

22. Conclusion

This thesis tried to shed some light on the wide range of gear types, the various parameters that define a gear tooth profile and the procedure to constructing that profile in a way such that the gear can fulfill its function of having a constant angular velocity ratio.

After a short description of various forming techniques, the bulk content of the thesis details applications of forming by shaping for external spur gears, internal spur gears, helical gears and face-gears. These applications are the first step in generating the profile on the blank gear that is the envelope of the cutter movement positions. That procedure was developed for internal spur gears.

The fillet correction that has been used is empirical rather than theoretical but it gives in relatively acceptable results as far as the scope of the thesis is concerned. Better fillet enhancement could be made, with a deeper theoretical background in play.

This envelope generating procedure can also be adopted and modified accordingly to accommodate the other aforementioned gear types.

23. References

- Section 1: On the Origin of Clockwork, Perpetual Motion Devices, and the Compass
  Derek J. de Solla Price
  Page 84
  Design of Machinery – Third Edition
  Norton, Robert L.
  Page 462
  Gearing in the Ancient World. Endeavour
  Lewis, M. J. T.
  The Book of Knowledge of Ingenious Mechanical Devices
  Donald Hill
  Page 273
  Economic of Medieval India, 1200-1500
  Irfan Habib
  Page 53
  Science and Civilization in China: Volume 4, Part 2
  Joseph Needham
  Page 298
- Section 2: Shigley's Mechanical Engineering Design – Ninth Edition
  Richard G. Budynas and Keith Nisbett
  Chapter 13-2 Pages 675-676
- Section 3: Shigley's Mechanical Engineering Design – Ninth Edition
  Richard G. Budynas and Keith Nisbett
  Chapter 13-3 Page 677
  Machine Design: An Integrated Approach – Third Edition
  Norton, R.L.
- Section 4: Shigley's Mechanical Engineering Design – Ninth Edition
  Richard G. Budynas and Keith Nisbett
  Chapter 13-4 Page 678
- Section 5: Shigley's Mechanical Engineering Design – Ninth Edition
  Richard G. Budynas and Keith Nisbett
  Chapter 13-5 Pages 679-681
  Fundamentals of Machine Component Design – Fourth Edition
  Juvinall, R.C. and K.M. Marshek
  Page 598
  Open Gearing Catalog
  Boston Gear Company
- Section 6: Shigley's Mechanical Engineering Design – Ninth Edition
  Richard G. Budynas and Keith Nisbett
  Chapter 13-8 Pages 687-689
  Pictures: https://www.tec-science.com/mechanical-power-transmission/involute-gear/gear-cutting/

- Section 7: Shigley's Mechanical Engineering Design – Ninth Edition
  Richard G. Budynas and Keith Nisbett
  Chapter 13-6 Pages 684-685
- Section 8: Shigley's Mechanical Engineering Design – Ninth Edition
  Richard G. Budynas and Keith Nisbett
  Chapter 13-12 Pages 696-697
  AGMA 913 standards – American Gear Manufacturers Association
- Section 9: Gear Geometry and Applied Theory – Second Edition
  Faydor L. Litvin and Alfonso Fuentes
  Chapter 1-5.2 Pages 17-19
- Section 11: Gear Geometry and Applied Theory – Second Edition
  Faydor L. Litvin and Alfonso Fuentes
  Chapter 1-5.3 Pages 19-20
- Section 13: Shigley's Mechanical Engineering Design – Ninth Edition
  Richard G. Budynas and Keith Nisbett
  Chapter 13-10 Pages 691-693
  Gear Geometry and Applied Theory – Second Edition
  Faydor L. Litvin and Alfonso Fuentes
  Chapter 14- 'Lines of Contact', 'Relation between Design Parameters'
  Pages 388,390-392
- Section 14: Gear Geometry and Applied Theory – Second Edition
  Faydor L. Litvin and Alfonso Fuentes
  Chapter 1-5.1 Pages 15-17
- Section 16: Gear Geometry and Applied Theory – Second Edition
  Faydor L. Litvin and Alfonso Fuentes
  Chapter 1-5.5 Pages 22-24
- Section 18: Gear Geometry and Applied Theory – Second Edition
  Faydor L. Litvin and Alfonso Fuentes
  Chapter 18-1,2,3,4 Pages 508-514
- Section 19: Gear Geometry and Applied Theory – Second Edition
  Faydor L. Litvin and Alfonso Fuentes
  Chapter 18-5 Pages 517-518
- Section 21: Gear Geometry and Applied Theory – Second Edition
  Faydor L. Litvin and Alfonso Fuentes
  Chapter 6-9 Pages 119-121